Earth-Science Reviews 169 (2017) 180–201

Contents lists available at ScienceDirect

Earth-Science Reviews

journal homepage: www.elsevier.com/locate/earscirev

Geothermal resources within carbonate reservoirs in western Sicily (Italy): A review

D. Montanari*, A. Minissale, M. Doveri, G. Gola, E. Trumpy, A. Santilano, A. Manzella

Institute of Geosciences and Earth Resources, National Research Council of Italy (CNR), Italy

ARTICLE INFO

Keywords:
Geothermal systems
Carbonate reservoirs
Temperature modeling
Fluid geochemistry
Groundwater flow paths
Sicily
Structural geology
Italy

ABSTRACT

Low-to-medium temperature fluid reservoirs hosted in carbonate rocks are some of the most promising and unknown geothermal systems. Western Sicily is considered a key exploration area. This paper illustrate a multidisciplinary and integrated review of the existing geological, geochemical and geophysical data, mainly acquired during oil and gas explorations since the 1950s, specifically re-analyzed for geothermal purposes, has led to understanding the western Sicily geothermal system as a whole, and to reconstructing the modalities and particular features of the deep fluid circulation within the regional reservoir. The data review suggests the presence of wide groundwater flow systems in the reservoir beneath impervious cap rocks. We identified the main recharge areas, reconstructed the temperature distribution at depth, recognized zones of convective geothermal flow, and depicted the main geothermal fluid flow paths within the reservoir.

We believe that our reconstruction of geothermal fluid circulation is an example of the general behavior of low-to-medium enthalpy geothermal systems hosted in carbonate units on a regional scale. Due to the recent technological developments of binary plants, these systems have become more profitable, not only for geothermal direct uses but also for power production.

1. Introduction

With the exception of active volcanic areas where geothermal reservoirs are generally hosted in permeable volcanic horizons (e.g., Henley and Ellis, 1983; Moeck, 2014), deep carbonate aquifers host what are probably the most important geothermal resources in the world (e.g.; Gousmania et al., 2006; Homuth et al., 2015; Minissale and Duchi, 1988; Mohammadi et al., 2010; Pasquale et al., 2014; Simsek, 2003). Within karstified carbonates, widespread fracture systems generally play an important role in geothermal fluid flows, both as recharge and discharge, such as occurs in the high-enthalpy Larderello-Travale geothermal field in Italy, the most famous high-enthalpy reservoir hosted in carbonates units (e.g., Bertini et al., 2006; Minissale, 1991; Romagnoli et al., 2010; Sani et al., 2016).

The features and behavior of these high temperature systems are uncommon because of the exceptional nature of the heat source, however they are fairly well known due to the great economic interest in these resources, and their longtime exploitation. On the other hand, low-to-medium temperature reservoirs (i.e. below 150 °C) are widespread, but much less understood. These geothermal systems are not strictly related to an individual heat source and thus they can be characterized by much greater extent. Because of the high permeability and storage and drainage capacity of limestones and dolostones, these systems are very favorable targets, also on a regional scale, for exploiting geothermal energy. These geological units often host significant low-to-medium temperature resources, and can be found, for example, in central Europe (Goldscheider et al., 2010 and references therein) and China (Duan et al., 2011).

These kinds of reservoirs are already exploited both for electric power generation and district heating. Table 1 reports a list of applications in central Europe. These low-to-medium temperature applications are still not well developed worldwide because research has been mainly targeted at high temperature systems suitable for producing electricity.

In Italy, low-to-medium temperature systems are underdeveloped, despite the huge geothermal potential (Trumpy et al., 2016; Cataldi et al., 1995). There is only one good example of the use of such carbonate circulating fluids for space heating near the city of Ferrara in northern Italy (Gianbastiani et al., 2014). Mesozoic carbonate rocks constitute the backbone of the Italian peninsula, as well as western Sicily, which is a natural laboratory for the study of these low-to-medium temperature geothermal systems.

We choose western Sicily as a key area because, from a geothermal point of view, Sicily (Fig. 1) is a very stimulating area characterized by

* Corresponding author.
E-mail address: domenico.montanari@igg.cnr.it (D. Montanari).

http://dx.doi.org/10.1016/j.earscirev.2017.04.016
Received 21 December 2016; Received in revised form 21 March 2017; Accepted 29 April 2017
Available online 03 May 2017

Table 1
Example installations in Central Europe currently producing geothermal energy from carbonates (modified after Goldscheider et al., 2010). The Ferrara data from http://geodh.eu/project/ferrara/. NA not applicable, ND no data available.

Location	Production T (°C)	Well depth (m)	Installed capacity (MW)
Altheim (Austria)	106	2300	11.5
Bad Blumau (Austria)	110	2843	7.6
Bad Waltersdorf (Austria)	63	1400	2.3
Ferrara (Italy)	105	1100	14
Geinberg (Austria)	105	2225	7.8
Simbach Braunau (Austria)	81	2200	9.3
Paris Basin (France)	50–85	1400–2000	NA
Riehen (Switzerland)	66	1547	3.6
Erding (Germany)	65	2350	8
Pullach (Germany)	107	3443	6
Riem (Germany)	93	2746	9
Unterföhring (Germany)	86	2512	ND
Unterhaching (Germany)	123	3346	40
Unterschleissheim (Germany)	81	1960	13

the presence of: i) several thermal manifestations at the surface some of which are used for balneotherapy (Alaimo et al., 1978,; Caracausi et al., 2005; Favara et al., 1998; Favara et al., 2001), ii) localized areas of moderately high heat flow (Della Vedova et al., 2001) and iii) thick carbonate units extending from the surface down to great depths (Catalano et al., 2013 and references therein; Montanari et al., 2015).

In the southernmost part of the study area, several hydrocarbon exploration wells, drilled since the 1950s, have provided new geological data to define the geometric relationships between the tectonic units above the limestones and the structural reconstruction at depth (Catalano et al., 1995; Catalano et al., 1998; Catalano et al., 2002). In addition, a great amount of seismic, well-log data (i.e., thermometric, sonic, gamma-ray) and geochemical data have been useful for assessing regional geothermal resources.

According to a geothermal perspective, we reviewed the data that were also integrated with geological surveys, and new geochemical data collected at surface on a large number of thermal springs. The multidisciplinary and integrated work presented here enabled us to decipher the functioning of the regional-scale geothermal system which, in our opinion, could be taken as an example for many other similar geothermal systems worldwide. Our objective is also to stimulate and promote research into these low-to-medium temperature systems, since they represent one of the most readily-exploitable conventional geothermal sources (e.g. Trumpy et al., 2016).

2. Geological and geothermal background

The western Sicily fold and thrust belt connects central and eastern Sicily to the Late Cenozoic Maghrebian submerged chain developing along the African-European plate boundary (Fig. 1). This chain involves a complex architecture of thrust systems resulting from a deformation history which has been active since Oligocene-early Miocene times (e.g. Barreca and Maesano, 2012; Bello et al., 2000; Catalano et al., 1996; Catalano et al., 2002; Catalano et al., 2013; Di Stefano et al., 2015; Lentini et al., 1994; Monaco et al., 1996).

Western Sicily is constituted at depth by Mesozoic carbonate platforms and their clastic covers, which are Cretaceous to Miocene in age. From a structural point of view this portion of the chain is characterized in the northern sector by a tectonic stack of units up to 12 km thick (Catalano et al., 2002) and by a less deformed southern sector, but still affected by shortening (Barreca et al., 2014). Consequently, in the northern portion of western Sicily, carbonate platform units and covers extensively crop out as they are involved in a regional structural high, whereas, to the southeast, these units are encountered only in deep wells drilled for oil exploration (Figs. 1, 2 and 3).

The tectono-stratigraphic assemblages, now exposed in the western Sicily chain, are derived mainly from carbonate platforms and intervening basins lying on a sector of the Mesozoic African margin (Catalano et al., 1996). Various stratigraphic and tectonic studies in Sicily have confirmed that these Paleozoic-Mesozoic to Miocene units represent the sedimentary cover of distinct paleogeographic domains (locally named Imerese, Sicanian and Pre-Panormide, Panormide, Trapanese, Saccense and Iblean-Pelagian). These domains belonged to the Pelagian/African continental margin and to the “Tethyan” ocean branch prior to the onset of the deformation (Catalano et al., 2000 and reference therein; Bernoulli, 2001). Clastic-terrigenous Miocene-Pleistocene rocks deposited in foreland and wedge-top basins during the deformation of the continental margin domains cover these carbonate rocks, acting as a cap rock for the geothermal system at depth. For the stratigraphic characteristics of the different units exposed in Sicily, see Fig. 2 in Montanari et al., 2015.

These units are assumed to lie on top of the possibly Pan-African crystalline basement (Vai, 2001; Finetti et al., 2005; Accaino et al., 2011).

Western Sicily is bordered to the south by the Sicily Channel (Fig. 1) connecting the western and eastern parts of the Mediterranean Sea (Corti et al., 2006; Belguith et al., 2013 and references therein). This is a tectonically complex area where different unrelated geodynamic processes such as rifting and mountain building interact at the same time. In the Sicily Channel (Fig. 1) magmatism has been active since the Miocene age (Civetta et al., 1998) but is mainly associated with Pliocene-Pleistocene rifting (Corti et al., 2006). The magmatism is concentrated mainly on the Pantelleria and Linosa volcanic islands (e.g. Avanzinelli et al., 2013). In addition, in 1831 on the Graham Bank the submarine volcano Empedocles gave rise to the ephemeral isle of Ferdinandea located between the isle of Pantelleria and Sciacca on the southern coast of western Sicily (Fig. 1). Many volcanic centers are also present in the Sicily Channel such as the Pliocene-Pleistocene Anfitrite and Tetide (Fig. 1), located in the Adventure plateau (Civile et al., 2016). The Sicily Channel is accordingly characterized by heat flow anomalies with maximum values on Pantelleria (Della Vedova et al., 2001). We have very little information on the Mediterranean sector between Pantelleria and Sciacca, however it is likely that the whole area is affected by a thermal anomaly and may contain unexplored geothermal systems connected with those in Sicily (e.g. Capaccioni et al., 2011).

Regarding the thermal springs emerging in western Sicily (Fig. 2), some are described in classical antiquity (e.g. the ancient Imera near the present Termini Imerese) and, around “Terme Segestane” a magnificent Greek temple highlighting the important role of thermal springs during the Greek domination of Sicily. Most thermal springs discharge along the seashore above or below sea level (Catalano et al., 1988), or at low elevations near the coast. Others emerge inland at relatively higher elevations, but always at the edges of the Mesozoic carbonate outcrops (Alaimo et al., 1978), near their contacts with terrigenous cover units. In addition to the evidence provided by the thermal springs, many measurements within oil and gas wells showed a positive heat flux (Fig. 1c) and temperature anomalies at depth along the coastal area, especially between Marsala and Agrigento (Cataldi et al., 1995; Fancelli et al., 1991).

A further element contributing to the geothermal favourability and potential (Trumpy et al., 2015; Trumpy et al., 2016) of the region, is the fact that the tectonic deformation in western Sicily is still quite active (e.g. Angelica et al., 2013; Barreca et al., 2014; Farolfi and Del Ventisette, 2015), as evidenced by historical and instrumental seismicity (Lavecchia et al., 2007). Southwestern Sicily is characterized by active shortening as dramatically testified by the 5.9 magnitude destructive earthquake occurring in the Belice valley in 1968 (Monaco et al., 1996). Archaeoseismological studies also indicate that the ancient Greek colony of Selinunte located in between Mazara del

Fig. 1. a) Simplified tectonic map of Sicily and central Mediterranean (modified according to Catalano et al., 2013). b) Location of the studied area (modified from Google Earth). c) Heat flow map of Sicily (redrawn from Della Vedova et al., 2001 and Google Earth).

Vallo and Sciacca, was destroyed between 370 and 300 BCE (Bottari et al., 2009), thus providing evidence that the 1968 earthquake was not an isolated event for the area. Through analysis of satellite images, observations by Barreca et al. (2014) provide additional evidence of active thrusting in SW Sicily and the Sicily Channel.

Active extensional tectonics affect the northern sector of the study area, related to the geodynamics of the southern Tyrrhenian back-arc basin.

Active tectonic deformation significantly contributes to the geothermal fluid flows in the region since it keeps the fractures open, dynamically sustaining effective permeability within the reservoir both upwards and downwards (e.g.; Bjornsson et al., 2001; Curewitz and Karson, 1997; Sibson, 1996).

3. Characterization of the geothermal circulation of fluids in western Sicily

In order to identify the main characteristics of the geothermal systems in western Sicily, all geological, hydrogeochemical and geophysical data from the literature were selected and critically revised. As a starting point we reviewed the datasets from the first attempt to evaluate the geothermal potentialities of Sicily, performed by the National Research Council of Italy, within the framework of the inventory of geothermal resources promoted in the 1980s by the Italian Ministry of the Industry (Catalano et al., 1982; Fancelli et al., 1991; Fancelli et al., 1994). These previous studies identified the main geothermal reservoir within the Mesozoic carbonatic units (e.g. Fancelli et al., 1991), the top of these units being recently mapped on a regional

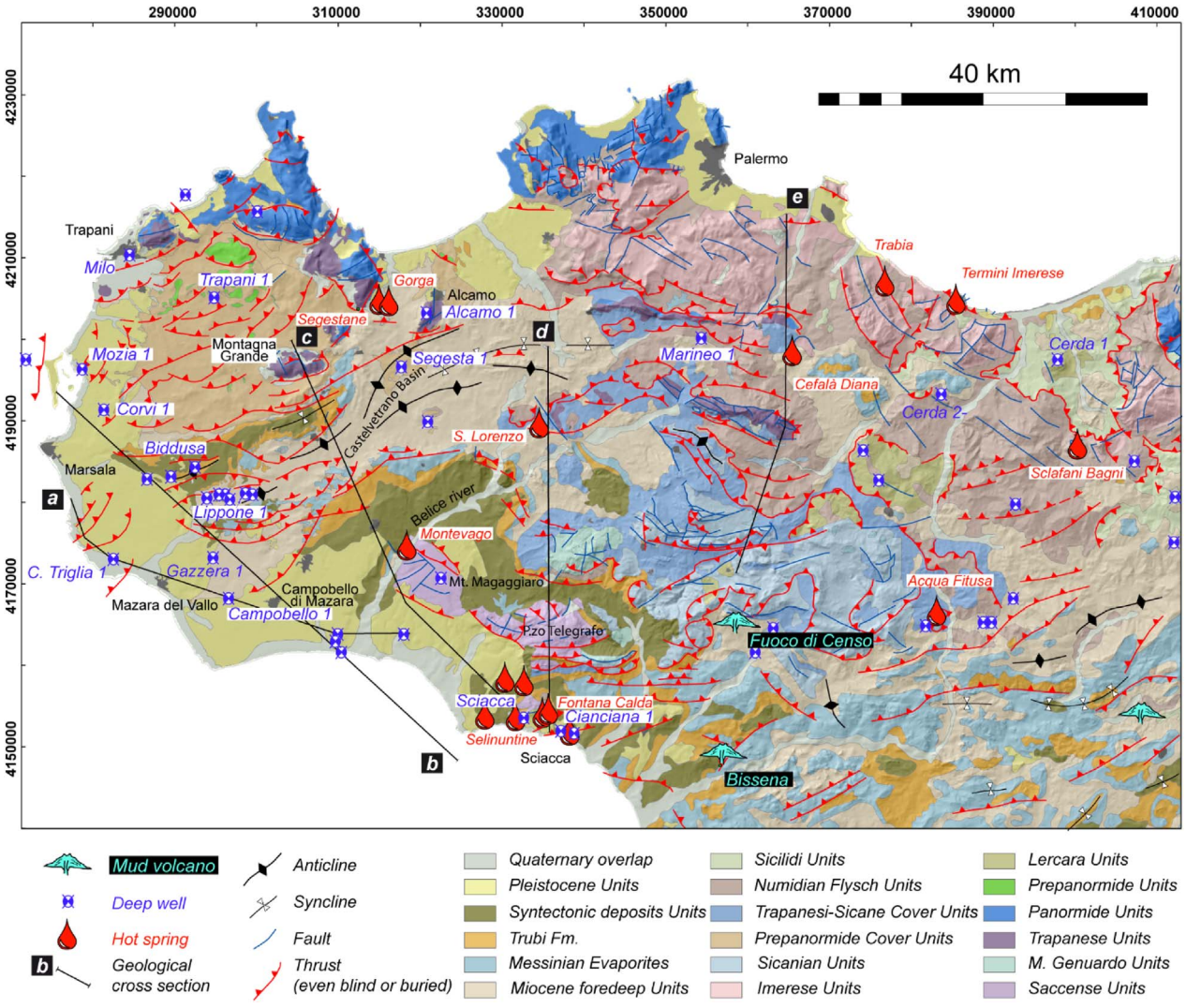

Fig. 2. Geological map of western Sicily, the location of geothermal manifestations and deep wells are also reported (modified from Abate et al., 2015).

scale (Montanari et al., 2015). We updated the datasets with new data from the literature and the Italian National Geothermal Database (Geothopica, 2012), together with new data gathered in the present study. The Italian Geothermal Database (Trumpy and Manzella, 2017) was recently updated with information from oil and gas boreholes (mostly well-log data) from the Italian Oil Co (AGIP, now ENI S.p.A.), and published by the Ministry of Economic Development.

3.1. Well-log data

Identifying and characterizing geothermal reservoirs draws on techniques common to petroleum exploration. To constrain the geothermal system and assess the petrophysical properties to the main lithological units, we used exhaustive lithostratigraphic data, borehole geophysical logs, drill-stem tests, core analyses and technical drilling information, e.g. lost circulation during drilling and drilling mud weights, from several hydrocarbon exploratory wells. A lithological analysis identified the deep-seated carbonate reservoir units, characterizing the thickness of the overlying sedimentary cover units acting as cap-rock. These units are constituted by Tertiary clay-rich siliciclastic sediments in which the well-log notes highlight a significant groundwater flow exclusively confined to the upper zone (generally within 200 m of depth from ground level). The well-log data analysis confirmed how thermal waters circulate exclusively within the Mesozoic carbonates units. Even where these units are overlain by Miocene limestones, the latter are not affected by significant water circulation with just very rare exceptions (Fig. 4 and Appendix A). The Mesozoic units consist of fractured limestones and dolostones whose fracture networks lead to the development of important groundwater flow systems (Fig. 4 and Appendix A).

To gain an insight into the thermal conductivity distribution at depth, a quantitative lithology characterization was performed, based on the processing of the combined responses of the gamma ray and sonic logs recorded every meter along selected boreholes. We assumed that each specific tool response varies in direct response to the proportion of each constituent of the bulk rock including pore-fluids (Fisher et al., 1992). We chose to solve for idealized pure lithologies with average properties rather than individual mineral components. In the cover units, we solved the petrophysical model for the volume fraction of porosity, shale and sandstone. We assumed a sonic velocity of 300 μs/ft and 60 μs/ft and a gamma ray radiation of 170 API units and 30 API units for shales and sandstones, respectively. In the reservoir units, for the porosity, we investigated limestone and dolostone volume fractions.

We assumed a sonic velocity of 46 μs/ft and 44 μs/ft and a gamma ray radiation of 5 API units and 15 API units for limestones and dolostones, respectively. The pore-filling fluid was assumed to be salt water with a sonic velocity of 185 μs/ft and a negligible gamma ray radiation.

Well logs also provided very useful temperature data measured

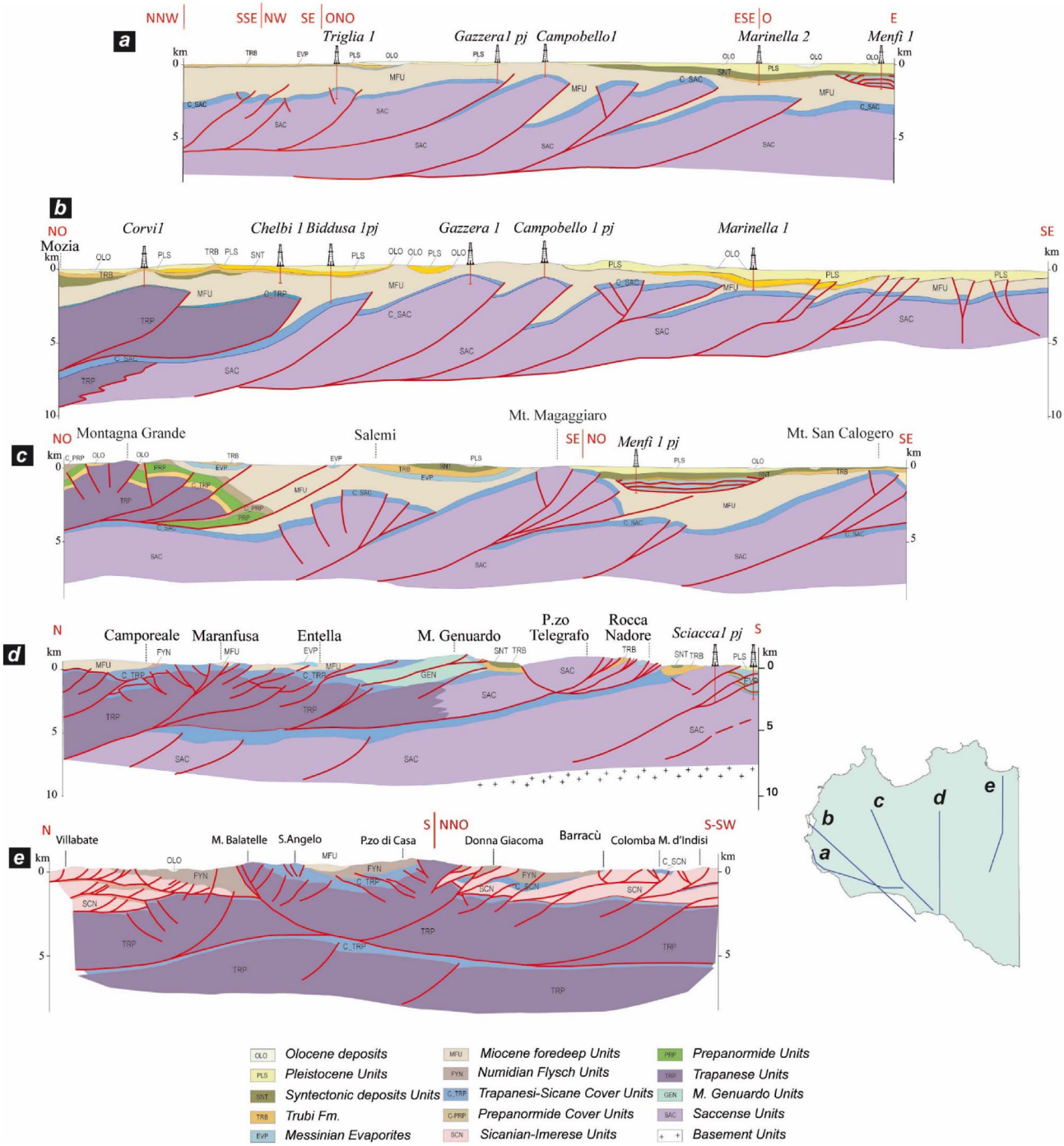

Fig. 3. Geological cross sections showing the structural geometries at depth. Locations are also reported in Fig. 2 (modified from Abate et al., 2015). The geological cross-sections were mainly built from field data collected at surface, deep wells, published seismic reflection profiles (e.g. Catalano et al., 1995; Catalano et al., 1998; Catalano et al., 2002) and unpublished seismic profiles kindly provided by Eni S.p.A, in the frame of the Vigor project.

within the reservoir. This thermal data, mainly bottom-hole temperatures (BHT) (Fig. 4 and Appendix A), were corrected for the thermal effects due to the drilling (Pasquale et al., 2008; Trumpy et al., 2015).

When time-temperature series of BHTs from the same borehole and depth interval were measured, we applied the well-known Horner method (Lachenbruch and Brewer, 1959) to extrapolate the static bottom-hole temperature (SBHT). Otherwise, when only single couples of BHT and related shut-in time (Δt) were available, we employed a technique that enable to correct single BHT-Δt data as function of the measurement depth and Δt (Pasquale et al., 2012 and references therein). This empirical correction based on the roughly proportionality between the slope of the regression line in the Horner plot and the strength of the heat supplied to the borehole per unit length and unit time as function of depth. We calibrated our empirical depth-time correction by a 2nd-order polynomial regression through the Horner-slope data evaluated over a broad area in Southern Italy (Gola et al., 2013; Trumpy et al., 2016). The analysis of temperatures measured inside the regional geothermal reservoir enabled us to identify distinct thermal signatures within the different parts of reservoir moving from the feeding areas (Montagna Grande-Alcamo to the North and Mt. Magaggiaro to the Southeast) towards the distal southwestern sector (Fig. 5). On and near to the outcropping carbonate units, the measured temperatures defined an average geothermal gradient of about 10 °C/km (yellow circles in Fig. 5) with a surface intercept very close to the

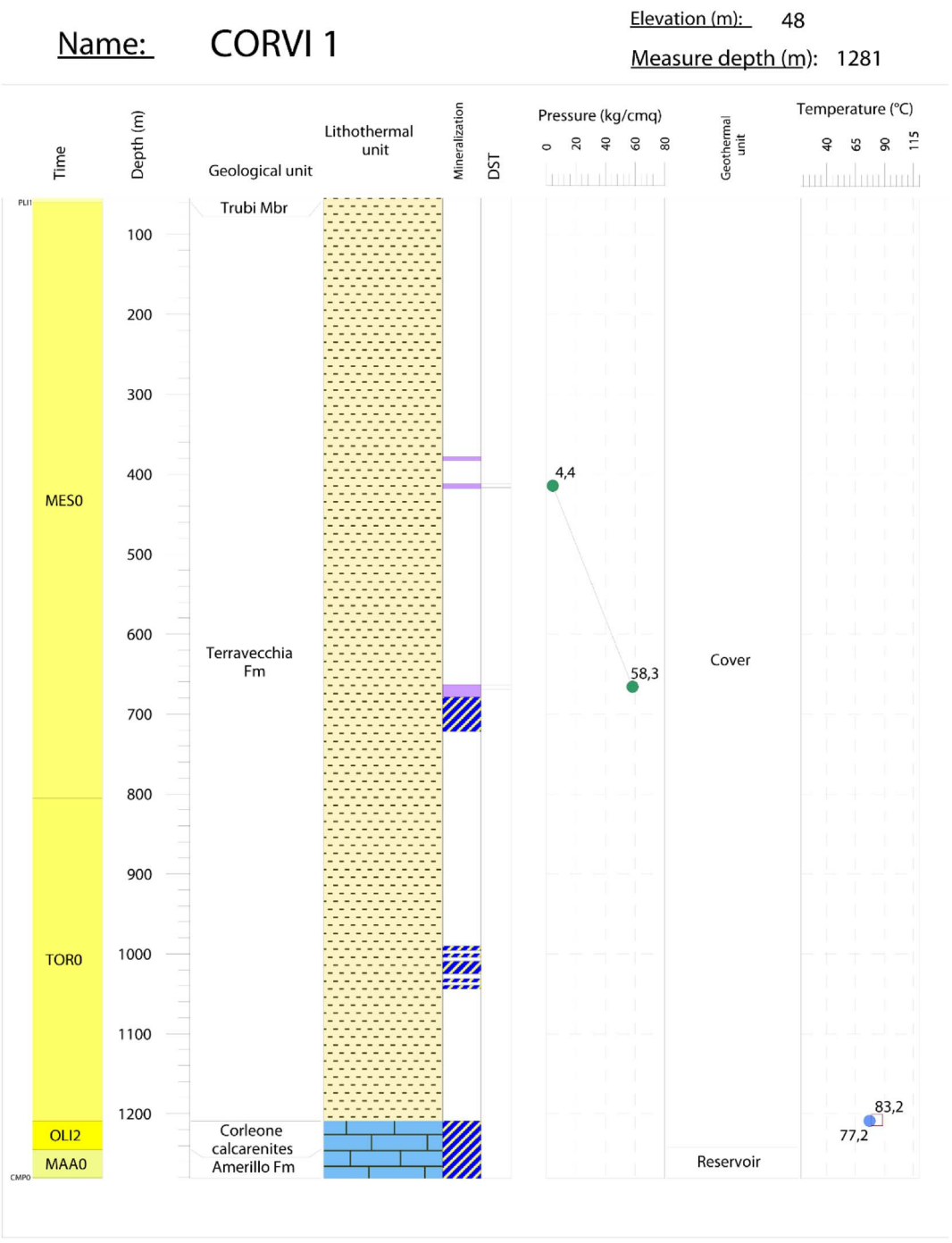

Fig. 4. Example of compiled well data sheet; symbol legend as in Appendix A.Example of compiled well data sheet; symbol legend as in Appendix A.

measured data at shallow depth (blue circles in Fig. 5). The shallow section has an average temperature of 35 °C at 300 m below ground level, the latter coinciding approximately to the water table depth in the above-mentioned outcropping sites. In the southwestern sector, we still observed inside the reservoir a low geothermal gradient of 11 °C/km (red circles in Fig. 5), but the average temperature of the deep-logged section increased from 60 °C, measured in the proximal parts of the system, up to 95–100 °C in the distal one. A formation temperature > 100 °C was measured in the Contrada Triglia1 well near Mazara del Vallo, at 2200 m below ground level. Among many factors controlling the convective heat transport (e.g. the regional heat flow, the permeability and the thickness of the reservoir unit and physical heterogeneity within it), also the distance from the recharge areas seems to control the thermal setting within the regional reservoir. The infilling meteoric fluids cooled the temperature profiles in the sectors close to the outcropping reservoir. Moving out from the feeding areas, the heat flow from the underlying basement warms the circulating fluids and the resulting gravitational instability due to the initial geothermal gradient may trigger convection currents within the water column. The latter process seems to be at the origin of the surface heat flow anomalies observed in the distal part of the system, in the southwestern sector.

In 17 hydrocarbon exploration wells, the permeability was evaluated through an analysis of 29 drill-stem tests (DST) performed in the Mesozoic carbonate formations. The average depth of the tested intervals, with a typical thickness of about 35–40 m, ranged from 840 to 2920 m. Jointly, porosity and permeability values measured in the laboratory on > 370 carbonate deep core samples, ranging from a few

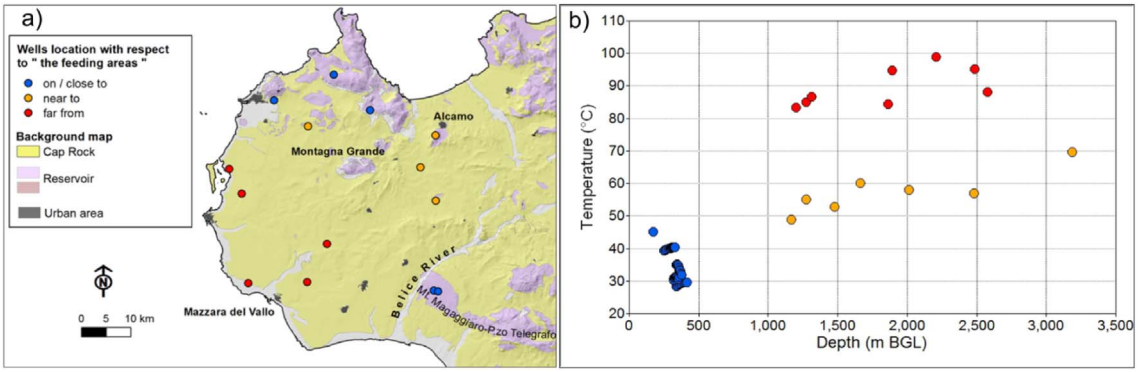

Fig. 5. Temperature measurements within the carbonate reservoir. a) Well location with respect to the zone where the carbonate units outcrop; b) temperature values vs. depth of measurement. (For interpretation of the references to color in this figure, the reader is referred to the web version of this article.)

hundred meters to over 6 km depth, were collected from 86 wells (data from ViDEPi Project: http://unmig.sviluppoeconomico.gov.it/videpi/progetto.htm) exploring analogous deep-seated carbonate platforms. Quantitative DST analysis assumed the following ideal conditions: i) single-phase radial flow, ii) homogeneous and infinite reservoir and iii) steady-state flow conditions.

The results displayed a relatively wide range of permeability from $1.9 \cdot 10^{-16}$ m^2 to $1.2 \cdot 10^{-13}$ m^2. Due to the basic assumptions and data quality, the permeability values obtained resulted in a first-order-of-magnitude estimation. Sources of uncertainty were i) the computed flow rate which could underestimate the true value because of the relatively short flow time in the DST, and ii) the estimation of the fluid viscosity under reservoir conditions. Laboratory measurements showed an average porosity of 6% with values varying from < 1% to over 30%. The high porosity values were more common in the dolomitized sections than in limestones. The average core permeability ranged from $< 1.0 \cdot 10^{-18}$ m^2 to $7.7 \cdot 10^{-13}$ m^2 measured on fine-grained dolostones and vuggy dolomicrites, respectively. Fig. 6 shows the permeability values as a function of the average depth of the tested and cored intervals.

The presence of fractured intervals was also evidenced by the lost circulation data. Both partial and total lost circulation were observed. Several situations can result in lost circulation, e.g. formations with an inherently high permeability or inappropriate drilling conditions.

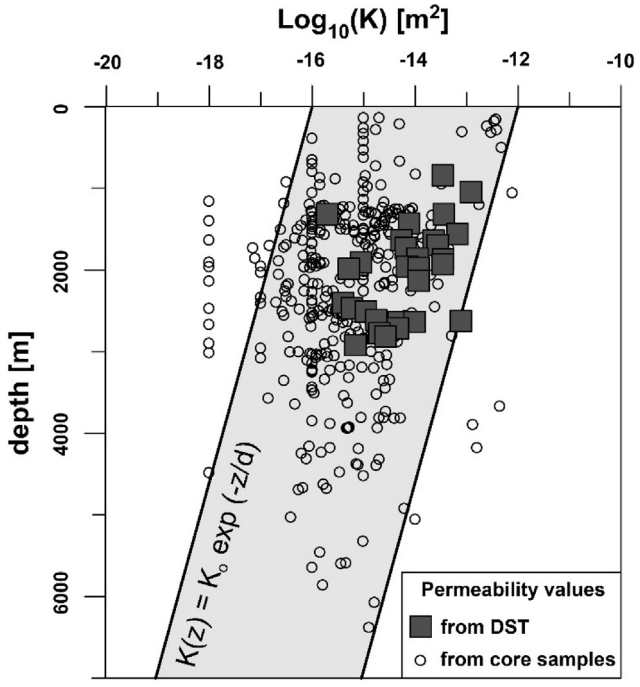

Fig. 6. Permeability values as a function of the average depth of the tested and cored intervals.

3.2. Geochemistry of natural thermal water and methane manifestations

In the western sector of Sicily both thermal springs and CH_4-rich gas manifestations associated with mud volcanoes (locally known as "*macalube*") are present (Figs. 1 and 2). Some thermal springs are located at low elevation near the coast (Termini Imerese, Selinuntine); a few emerge inland at relatively high elevations (Sclafani Bagni: 430 m; Cefalà Diana: 380 m); others are located along the Neogene basins at the foot of Mesozoic limestone outcrops (Segestane, San Lorenzo and Montevago springs, the latter also called Acqua Pia, Acque Calde and Vuturo in the literature), see Fig. 7 for thermal springs location. Most have been analysed on a regional scale in the past century (Alaimo et al., 1978, 1990; Dall'Aglio, 1966; Dall'Aglio and Tedesco, 1968; Carapezza et al., 1977; Fancelli et al., 1991, 1994; Favara et al., 1998; Gino and Sommaruga, 1953) as well as this century (Favara et al., 2001; Grassa et al., 2006). Some detailed studies for singular emission areas have also been carried out locally, especially at Termini Imerese and Selinuntine, respectively (Alaimo, 1984a, 1984b; Alaimo and Tonani, 1984; Antolini and Sommaruga, 1953; Aureli, 1996; Capaccioni et al., 2011).

Apart from natural thermal emergences where good data sets are available, scattered and incomplete analyses of fluids from oil wells (ENI S.p.A.) (Fig. 2 for location) analysed at the end of drilling (mostly from 1955 to 1961) and included in the Italian Geothermal Database, were considered in the present review. Table 2 shows all the available data from the literature and new unpublished data for the Termini Imerese area. The main components for both springs and wells are plotted in the Langelier-Ludwig diagram in Fig. 8. The diagram shows four main groups: i) low-salinity (< 1 g/L) Ca-HCO_3 and Ca(Na)-HCO_3(Cl)type waters for the Cefalà Diana, Trabia and Fontana Calda (Sciacca) springs, ii) intermediate salinity (> 1, < 2,5 g/L), Ca-SO_4-type for the Segestane and Montevago springs and iii) Na-Cl(HCO_3) for the Acqua Fitusa spring, and iv) high salinity (> 10 g/L) Na-Cl type for the remaining samples including the near the coast emergences of Selinunte and Termini Imerese, the Sclafani spring and all the deep oil wells (Biddusa, Cerda 1, Contrada Triglia 1, Gazzera 1, Lippone 1, Sciacca and Milo; see locations in Fig. 7).

As already reported in other research on the Sicilian thermal springs (e.g. Alaimo et al., 1978), group i) comprises springs with relatively short circulation path in the local thermal anomalous area, group ii) has the typical composition of waters with a regional circulation in limestones and dolostones not only in Sicily but the entire Italian peninsula (Lotti, 1910), group iii) is represented by the Acqua Fitusa sample with a likely local Na-HCO_3 signature not necessarily related to a real deep thermal aquifer due to the relatively low emergence temperature, group

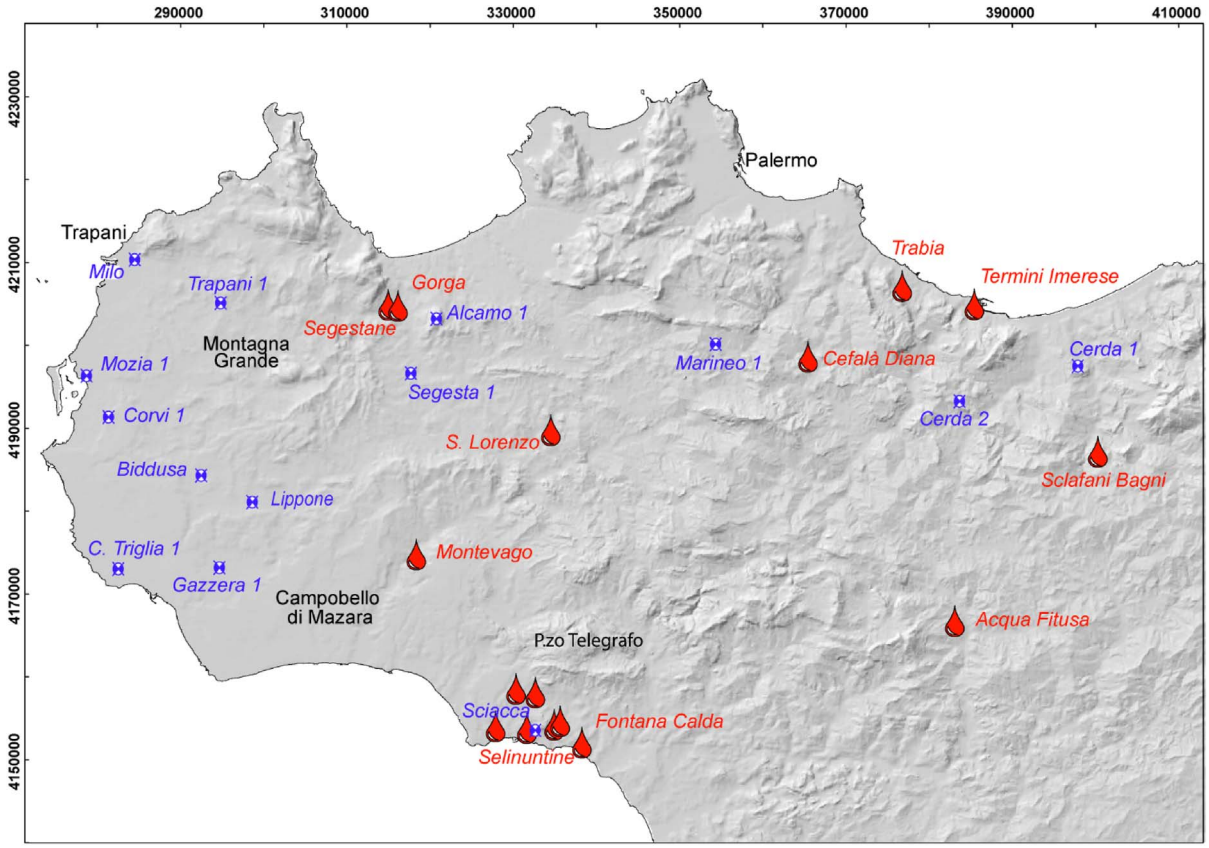

Fig. 7. Location of the thermal springs, deep wells described in Section 3.2.

iv) is characterized by the presence of sea water in their circuits and/or formation waters and/or halite horizons in the Neogene sediments (Alaimo et al., 1978; Fancelli et al., 1991; Favara et al., 1998, 2001; Grassa et al., 2006).

To highlight the origin of the water feeding the hydrothermal circuits in western Sicily in terms of their isotopic composition, Fig. 9 shows a multiple δD-δ^{18}O, δD-elevation, δD-Cl and δ^{18}O-Cl. From the δD-δ^{18}O diagram (a: top left), and as already commented on in the past (e.g. Favara et al., 2001; Grassa et al., 2006), it is evident that the Segestane, Montevago, Cefalà Diana, and Termini Imerese thermal springs and the water of the Milo well (the only deep oil well with available δD and δ^{18}O data), fall between or along both the Global Meteoric Water Line (GMWL: Craig, 1961) and the Local Meteoric Water Line (LMWL: Favara et al., 1998), the latter being very similar to the Mediterranean Meteoric Water Line as defined by Gat and Carmi (1970). Hence, the feed mainly occurs by meteoric water. By contrast, the thermal springs from Selinuntine, Sclafani and Acqua Fitusa show a significant shift from both the GMWL and the LMWL, especially for the hottest (56 °C) spring of the Selinuntine emerging near the town of Sciacca. The diagram in Fig. 9 suggests that the latter spring might be a mix between local meteoric waters and a shifted high-temperature Mediterranean Sea end-member, with a δ^{18}O of + 5.0 (‰ vs V-SMOW) as already proposed as a possible mixing process (Capaccioni et al., 2011; Grassa et al., 2006).

A similar mixing with a shifted seawater component has already been invoked in Sicily for the shallow aquifer present in the volcanic Islands of Vulcano (see Fig. 1 for location) (Bolognesi and D'Amore, 1993; Chiodini et al., 2000; Minissale, 1992) and Pantelleria (Doveri and Grassi, 2010; Duchi et al., 1994; Grassi et al., 1995; Parello et al., 2000). This process does not seem likely for the Selinuntine spring. In fact, a close examination of the δD-Cl diagram in Fig. 9c (bottom left) suggests a mixing between meteoric water and SMOW, as expected because hydrogen does not typically reacts with rock minerals and therefore is representative of the local altitude of recharge. The δ^{18}O-Cl diagram in Fig. 9d (bottom right), on the contrary, clearly suggests a mixing between a meteoric water end-member and the Mediterranean Sea. According to these two diagrams (Fig. 9c and d), the oxygen shift shown in Fig. 9a by the Selinuntine thermal spring must be related to an active hydrothermal system not necessarily related to the shifted Mediterranean Sea water, despite being shifted, as hypothesised by other authors (Capaccioni et al., 2011; Favara et al., 2001). This hypothesis, i.e. of a hydrothermal system present at depth, possibly offshore, not necessarily affected by the feeding of the Mediterranean Sea, is further corroborated by the analysis of trace elements in the thermal springs. As already reported by Favara et al. (2001), Br, Li, B etc., all are much higher than sea water (e.g. in the Br-Cl diagram in Fig.10) which clearly suggests prolonged water-rock interaction underground.

The remaining diagram in Fig. 9 b, reports two lines of δD variation with elevation (lines 3 and 4) representing rainfall that infiltrates at different altitudes in the southern and northern sectors of W-Sicily, respectively. Such lines derive from literature data (Fancelli et al., 1991; Liotta et al., 2013), which refer to local cold springs, using the approach proposed in other areas of central Italy (Doveri and Mussi, 2014; Minissale and Vaselli, 2011). We coupled the altitude and the δD values of springs located close to the peak of local reliefs, likely representing the local groundwater isotopic signature, whose average feeding altitudes are slightly higher than the spring altitudes. Such springs, shown in Fig. 11, were selected according to the different isotopic features of rainfall registered by Liotta et al. (2013) in these two N and S sectors.

In order to estimate the average recharge elevations of the regional flow-paths, clearly excluding those springs affected by sea water mixing (i.e. Selinuntine and Termini Imerese springs), in Fig. 9b we plotted the thermal spring values and compared them with the respective feeding sectors (N and S) as deduced from local cold springs as described above.

Table 2
Chemical and isotopic composition of thermal springs in western Sicily from 1978 to 2016.

		Year	Elev m	t °C	pH	TDS ppm	Ca ppm	Mg ppm	Na ppm	K ppm	HCO_3 ppm	SO_4 ppm	Cl ppm	Sr ppm	F ppm	Br ppm	Li ppm	NH_4 ppm	B ppm	SiO_2 ppm	$\delta^{18}O$ ‰SMOW	$\delta^{2}H$ ‰SMOW	^{13}C-Dic ‰PDB
1	Segestane[a]	1978	48	45.0	6.9	1843	186	72	274	16	262	509	462	2.6				0.2		60	− 7.00	− 39.7	
1	Segestane[b]	1990	"	43.3	7.0	1727	209	65	264	17	256	471	419							27	− 7.13	− 40.4	
1	Segestane[c]	1994	"	43.8	6.8	1710	172	58	261	15	214	511	449		3.8	1.7	0.05			25	− 7.41	− 39.4	
1	Segestane[d]	1991	"	44.0	6.9	1729	179	61	234	8	235	584	398		2.9	1.6	0.05			25	− 7.30	− 38.0	
1	Segestane[e]	2006	"	44.2	6.8	1700	204	70	231	13	253	480	418		3.6	1.7				26	− 7.20	− 38.0	− 4.6
2	Segestane Gorga 1[a]	1978	38	49.8	6.9	2302	234	83	366	20	262	566	699	2.6				0.3		69	− 6.99	− 39.2	
2	Segestane Gorga 1[b]	1990	"	49.5	6.9	2137	246	75	368	20	250	514	637							27	− 7.15	− 41.4	
2	Segestane Gorga 1[c]	1994	"	50.7	6.7	1993	211	78	356	15	168	511	620		3.2	1.4	0.07			29	− 7.45	− 40.2	
2	Segestane Gorga 2[d]	1991	"	49.5	6.7	2098	216	65	342	11	259	518	653		3.6	2.1	0.04			29	− 7.20	− 38.0	
2	Segestane Gorga 2[e]	2006	"	49.6	7.2	2221	236	83	395	16	296	528	663		1.5	2.1					− 7.50	− 38.0	− 4.9
3	Segestane Gorga 2[a]	1978	38	48.6	6.9	1632	184	63	207	12	238	499	369	2.2				0.4		57	− 6.34	− 39.9	
3	Segestane Gorga 2[b]	1990	"	48.0	7.0	1533	202	59	202	14	238	460	332							26	− 7.14	− 42.4	
3	Segestane Gorga 2[c]	1994	"	48.4	6.6	1452	174	56	197	8	229	446	307		3.7	2.5	0.12			29	− 7.42	− 39.3	
3	Segestane Gorga 1[d]	1991	"	48.2	6.8	1581	226	57	186	8	235	453	381		3.8	1.0	0.05			29	− 7.20	− 36.0	− 4.4
3	Segestane Gorga 1[e]	2006	"	48.3	7.1	1588	177	56	220	12	238	500	351		4.4	1.2				28	− 7.50	− 39.0	− 4.4
4	Montevago Acqua Pia[f]	1966	162	31.0	7.0	1239	128	55	101	10	244	283	183		1.4				216	18			
4	Montevago Acqua Pia[a]	1978	"	37.6	6.9	1436	162	68	154	12	244	461	270	2.6				0.1		63	− 6.32	− 35.6	
4	Montevago Acqua Pia[b]	1990	"	37.0	7.0	1524	212	76	168	16	244	501	284							23	− 6.65	− 37.2	
4	Montevago Acqua Pia[d]	1991	"	41.0	7.0	1619	205	78	178	17	247	551	298	4.2	18.4	1.6	0.06			21	− 5.80	− 29.0	
4	Montevago Acqua Pia[e]	2006	"	39.2	6.9	1560	189	84	179	15	275	480	312		3.2	1.0				22	− 6.70	− 35.0	− 4.0
5	Selinuntine-Sciacca[a]	1978	25	56.1	6.0	22,398	1270	429	5713	359	525	504	13,497	58.0				4.6		39	− 0.42	− 18.0	
5	Selinuntine-Sciacca[d]	1991	"	56.2	6.0	25,017	1331	441	7169	376	549	501	14,349	59.0	7.7	192.0	1.92			40	− 1.20	− 16.0	
5	Selinuntine-Sciacca[e]	2006	"	54.0	6.4	22,685	1249	472	6494	337	470	739	12,777		7.2	118.0				22	− 1.70	− 14.0	− 2.2
5	Selinuntine-Sciacca[g]	2011	"	55.0	6.4	22,910	1181	404	6620	385	506	1050	12,600		1.2	155.0		7.8			− 0.90	− 23.4	− 0.2
6	Molinelli-Sciacca[a]	1978	40	32.2	6.3	14,296	756	293	3933	203	433	317	8236	34.3				2.6		89	− 1.75	− 22.9	
6	Molinelli-Sciacca[d]	1991	"	32.0	6.3	12,715	754	266	3508	194	371	290	7171	33.1	3.6	88.0	0.99			35	− 2.30	− 19.0	
6	Molinelli-Sciacca[e]	2006	"	32.1	6.4	10,947	603	220	3238	171	354	338	5938		5.9	38.0				41	− 3.70	− 22.0	− 0.5
6	Molinelli-Sciacca[g]	2011	"	34.0	6.2	14,660	816	295	3986	232	464	288	8579								− 1.80	− 22.9	
7	Font. Calda-Sciacca[a]	1978	122	31.0	7.4	887	102	35	90	12	305	139	149	1.3				0.1		54	− 4.22	− 26.4	
7	Font. Calda-Sciacca[b]	2011	"	33.0	6.7	846	107	32	102	16	348	130	110		0.6	0.5		0.2			− 2.80	− 29.9	− 2.4
8	Termini Imerese[h]	1931	3	42.5	7.7	14,944	600	382	4279	213	412	1087	7924			21.8				25			
8	Termini Imerese[a]	1978	"	42.3	6.8	14,446	518	340	4244	168	293	1022	7831	5.7				0.6		24	− 3.80		
8	Termini Imerese[e]	2006	"	41.3	7.0	12,685	471	291	3984	126	287	745	6736		18.0	27.2					− 3.90	− 19.00	− 3.7
8	Termini Imerese[i]	2012	"	42.4	7.0	15,138	558	356	4416	164	305	1075	8207	5.5	3.0	32.8	1.10	0.1	2	13	− 3.90	− 26.50	− 1.6
9	Sclafani[a]	1978	430	32.7	6.5	10,633	330	198	3307	55	427	43	6106	143.0				5.5		18	− 4.32	− 40.6	
9	Sclafani[e]	2006	"	32.6	6.7	9736	244	194	3242	60	281	214	5398		45.5	43.3				14	− 5.00	− 36.0	− 1.8
10	Cefalà Diana[f]	1966	380	38.0	6.8	543	64	16	37	5	262	32	33		4.5				64	26			
10	Cefalà Diana[a]	1978	"	35.6	7.1	474	62	18	35	4	268	43	43	0.9				0.2			− 7.05	− 42.0	
11	Acqua Fitusa[a]	1978	375	25.0	7.3	3223	60	18	920	20	933	470	746	0.9				0.9		54	− 3.25	− 32.1	
11	Acqua Fitusa[e]	2006	"	25.2	7.2	2664	25	14	805	18	799	254	738		6.5	4.7					− 4.50	− 31.0	− 1.5
12	S. Lorenzo	1966	190	31.0	7.2	615	68	35	32	4	256	115	36		3.9				48	17			
13	Trabia[a]	1978	120	26.0	6.9	537	46	28	51	4	299	48	43	1.3						18	− 7.10		
14	Milo well[b]	1990		40.5	7.3	4258	157	68	1260	68	409	406	1870							20	− 5.37	− 29.7	
15	Biddusa well (1075 m)[j]	1961	− 1120	56.0	7.7	31,668	660	220	11,300	133	230	220	18,900							5			
16	Cerda 1 well (1062 m)[j]	1960	− 1062	51.0	11.6	22,253	680	0	8450	177	960	790	11,190							6			
17	Triglia well (1900 m)[j]	1982	− 1900	95.0	7.2	12,887	357	76	3970	220	1098	1062	6069	11.6						24			
18	Gazzera well (1080 m)[j]	1956	− 1080	80.0	7.6	7800	330	60	2185	195	880	1060	3010							80			

(continued on next page)

Table 2 *(continued)*

		Year	Elev m	t °C	pH	TDS ppm	Ca ppm	Mg ppm	Na ppm	K ppm	HCO_3 ppm	SO_4 ppm	Cl ppm	Sr ppm	F ppm	Br ppm	Li ppm	NH_4 ppm	B ppm	SiO_2 ppm	$\delta^{18}O$ ‰SMOW	$\delta^{2}H$ ‰SMOW	^{13}C-Dic ‰PDB
19	Lippone 6 well (930 m)[j]	1959	− 930	40.0	8.1	18,530	150	70	6450	80	640	420	10,660							60			
20	Sciacca well (350 m)[j]	1954	− 350	55.0	6.2	23,213	1300	440	6440	273	700	510	13,490							60			
20	Sciacca well (1560 m)[j]	1955	− 1560	67.0	9.6	13,038	880	240	3565	273	130	530	7380							40			
20	Sciacca well (2700 m)[j]	1955	− 2700	76.0	6.8	24,277	1470	330	6900	507	690	800	13,490					53.0		90			
20	Mediterranean Sea[i]		0	20.0	8.0	35,195	411	1290	10,759	398	145	2712	19,348	8.1	1.3	65.0				5	1.33	9.8	

[a] Alaimo et al. (1978).
[b] Fancelli et al. (1994).
[c] Favara et al. (1998).
[d] Favara et al. (2001).
[e] Grassa et al. (2006).
[f] Dall'Aglio (1966).
[g] Capaccioni et al. (2011).
[h] Antolini and Sommaruga (1953).
[i] this study
[j] AGIP unpublished.

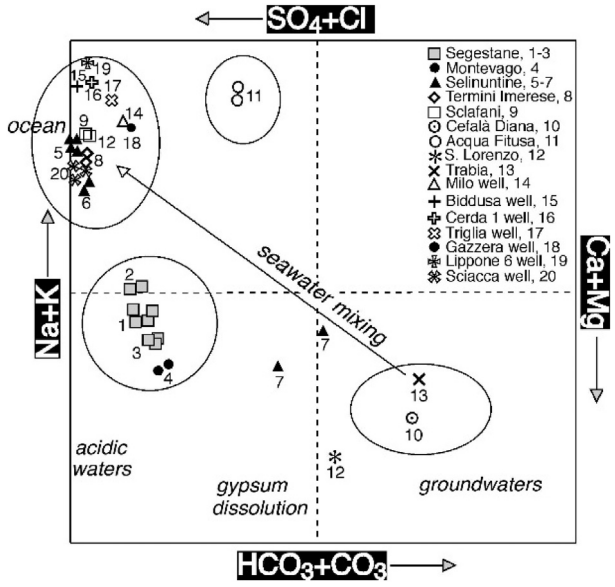

Fig. 8. Langelier-Ludwig diagram for the thermal samples investigated (see text for details).

The higher values of average recharge elevation are within the range of 600–750 m a.s.l., and refer to the springs of Segestane, Montevago and Cefalà Diana. For the Montevago spring, such average altitudes highlight how the recharge area also significantly extends into the inner part of the Sicani Mts (Fig. 11), where carbonate units widely crop out (Fig. 12).

Groundwater flows that originate from these mountainous zones extend for 30–40 km underground before flowing out at the spring sites. This thus demonstrates the regional character of the Mesozoic carbonate reservoir, at least in some sectors of W-Sicily, and its significant continuity beneath the impervious cover. This also agree with both the high flow rates (> 100–200 L/s; Dall'Aglio and Tedesco, 1968; Carapezza et al., 1977; Catalano et al., 1982; Monteleone and Pipitone, 1991) and the lack of tritium in the Segestane and Montevago springs (Fancelli et al., 1991), thus suggesting an apparent residence time of > 50 years. As regards the Acqua Fitusa spring, the average elevations of recharge water was about 400–500 m a.s.l., whereas for Fontana Calda (Sciacca) a value of about 200–250 m a.s.l. was obtained. Taking into account the location of these springs and the morphology in their surrounding zones (Fig. 11), such values could indicate a significant drainage of groundwater which originates locally, in agreement with the chemical-physical discussion.

As far as the gases associated with the singular thermal emergence areas in western Sicily are concerned, they clearly reflect the underground circuit. In general, there is a progressive increase in CO_2 and a simultaneous decrease in N_2 from the northernmost Segestane and Termini Imerese springs along the Tyrrhenian coast (both with N_2 > 90%), southwards to the Selinuntine emergences, where the CO_2 is over 90%. This difference is clearly related to a different ratio between descending meteoric, N_2-rich recharge water in the northern sector and deep, hot, CO_2-richer rising water, clearly increasing by moving southwards. The Sclafani, Cefalà Diana and Montevago springs, all located in between Segestane and Termini Imerese, have approximately 50% N_2 and 50% CO_2. As a matter of fact, If CO_2 points to a deep hot origin, possibly from an active hydrothermal system or the mantle at least in the Sciacca area according to the high $^{3}He/^{4}He$ ratio (R/Ra = 2.7) and a $\delta^{13}C$ of CO_2 in the mantle range (− 3.0 to − 6.0‰ PDB; Capaccioni et al., 2011), N_2 clearly reflects the recharge infiltrating water in the other emergencies. The warming up of the descending meteoric air-saturated recharge water, on a regional scale, lowers the solubility of nitrogen (oxygen is typically consumed in oxidative processes) which increases again towards the atmosphere as dissolved

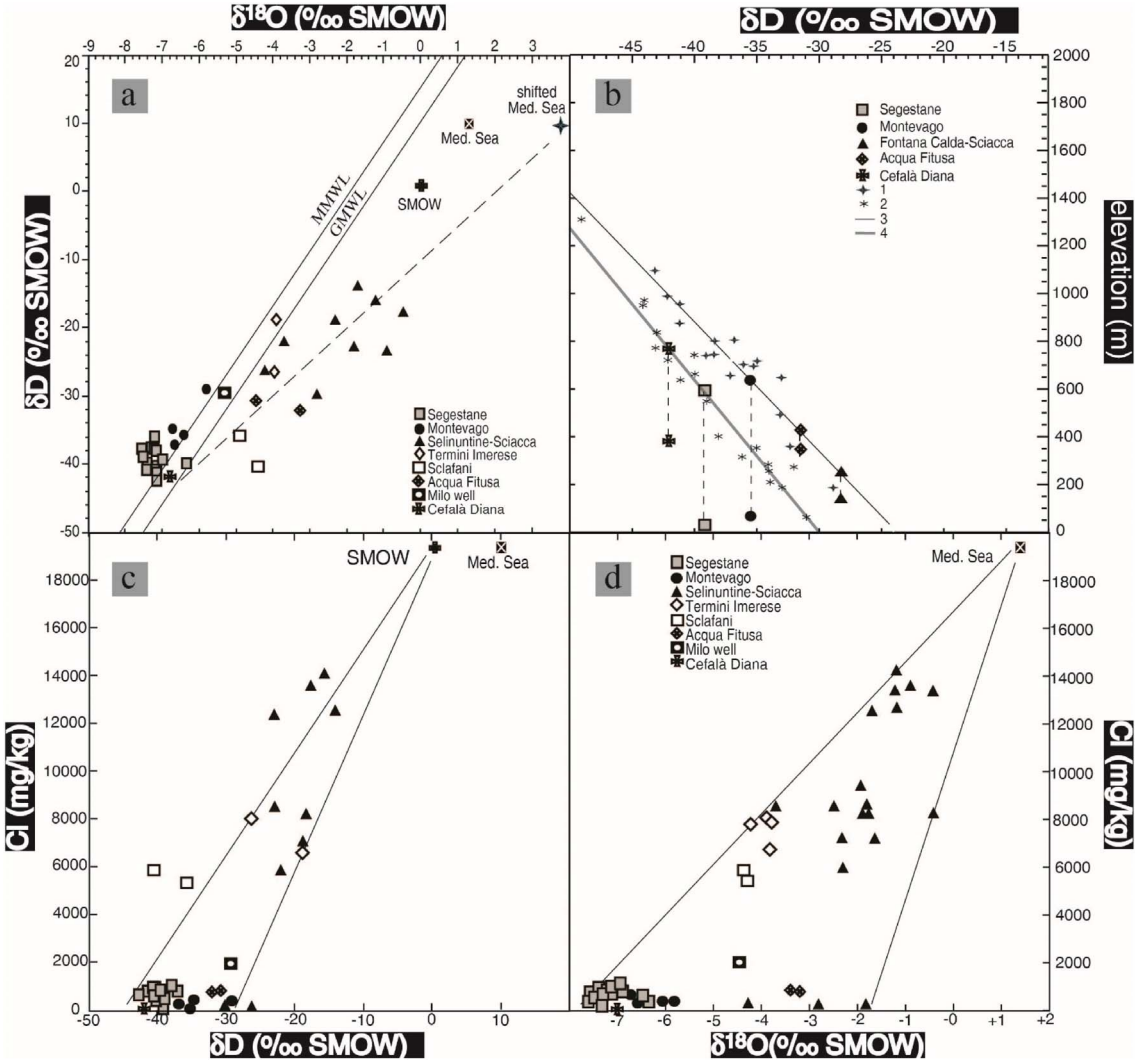

Fig. 9. Diagrams δD-δ^{18}O (a), δD-elevation (b): 1 - cold springs located in the southern sector of W-Sicily, data from Fancelli et al. (1991) and Liotta et al. (2013); 2 - cold springs located in the northern sector of W-Sicily, data from Liotta et al. (2013); 3 - regression line referring to points 1, "Elevation (m) = − 54.2 × δD‰ − 1278.6 [R2 = 0.89]"; 4 - regression line referring to points 2, "Elevation (m) = − 63.6 × δD‰ − 1902.0 [R2 = 0.97]"), δD-Cl (c) and δ^{18}O-Cl (d).

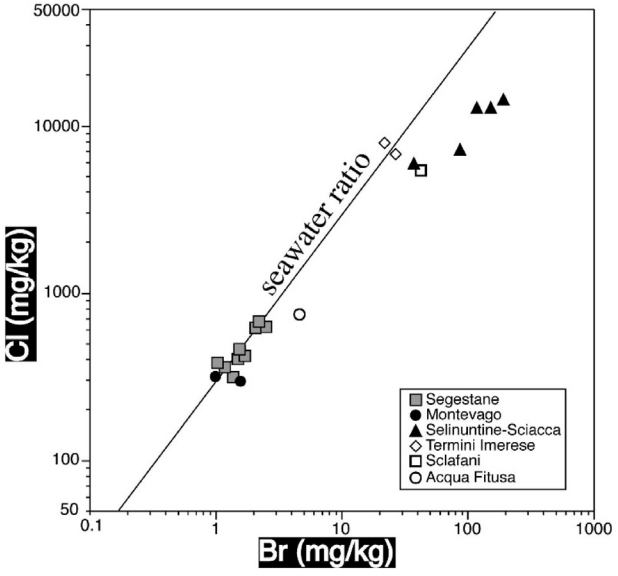

Fig. 10. Binary diagram of Cl vs Br for the thermal waters investigated showing a marked Br enrichment with respect to the seawater mixing line for the Selinunte-Sciacca samples.

free nitrogen in the hot rising water. The increase in CO_2 in the gas phase associated with the spring waters from the north to the south, is paralleled by a simultaneous increase in the $^3He/^4He$ ratio which peaks at the Selinuntine emergences near Sciacca. In a regional survey in western Sicily Caracausi et al. (2005) interpreted this feature as due to an outgassing through deep N-S extensional fault systems linked to the presence of mantle magmas intruded into the continental crust in western Sicily.

To complete the characterization of natural fluid emissions in western Sicily, the presence of CH_4 rich vents needs to be briefly discussed. In the 1950s, when oil was discovered in the Gela basin and the Sicily channel, the presence of the "*macalube*" at Bissena, Aragona and Fuoco di Censo (Figs. 1 and 2) was clearly related to marine sediments in the Caltanissetta basin (Fig. 1). It is reasonable to think that this prompted AGIP, the Italian oil company, to also carry out an exploration activity in western Sicily. Several wells were drilled up to 3000 m deep (Fig. 2) also near Sciacca, but no oil and only a little CH_4 was discovered (Videpi final well reports). Nevertheless, the $^3He/^4He$ ratio of 0.65 R/Ra measured at the *macalube* of Aragona (location in Fig. 1), without the presence of nitrogen, and therefore possible air contamination (R/Ra = 1 in air), suggests that the emission here is also affected by some mantle helium-3, as the R/Ra ratio is much higher than the expected value for a typical crustal gas enriched in ^4He (R/

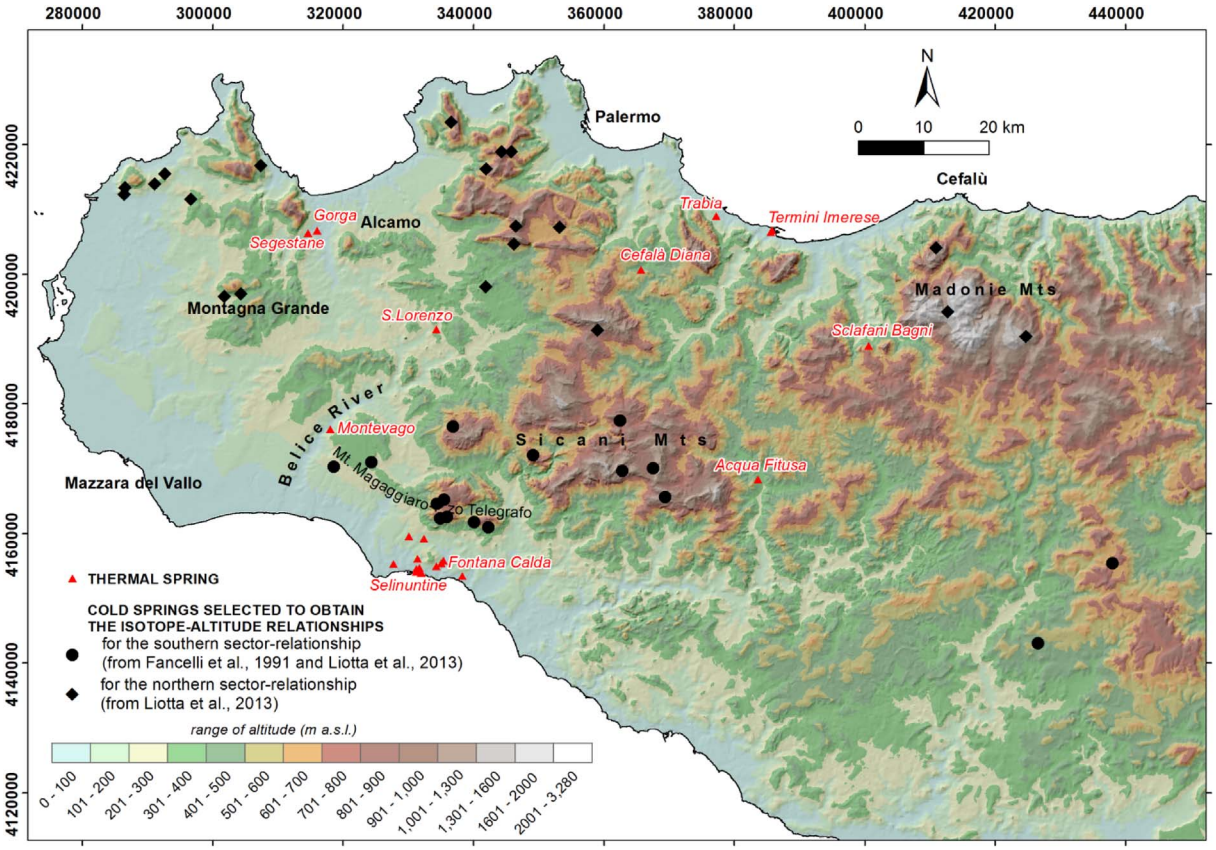

Fig. 11. Location of the thermal and cold springs used to obtain the isotope-altitudes relationships.

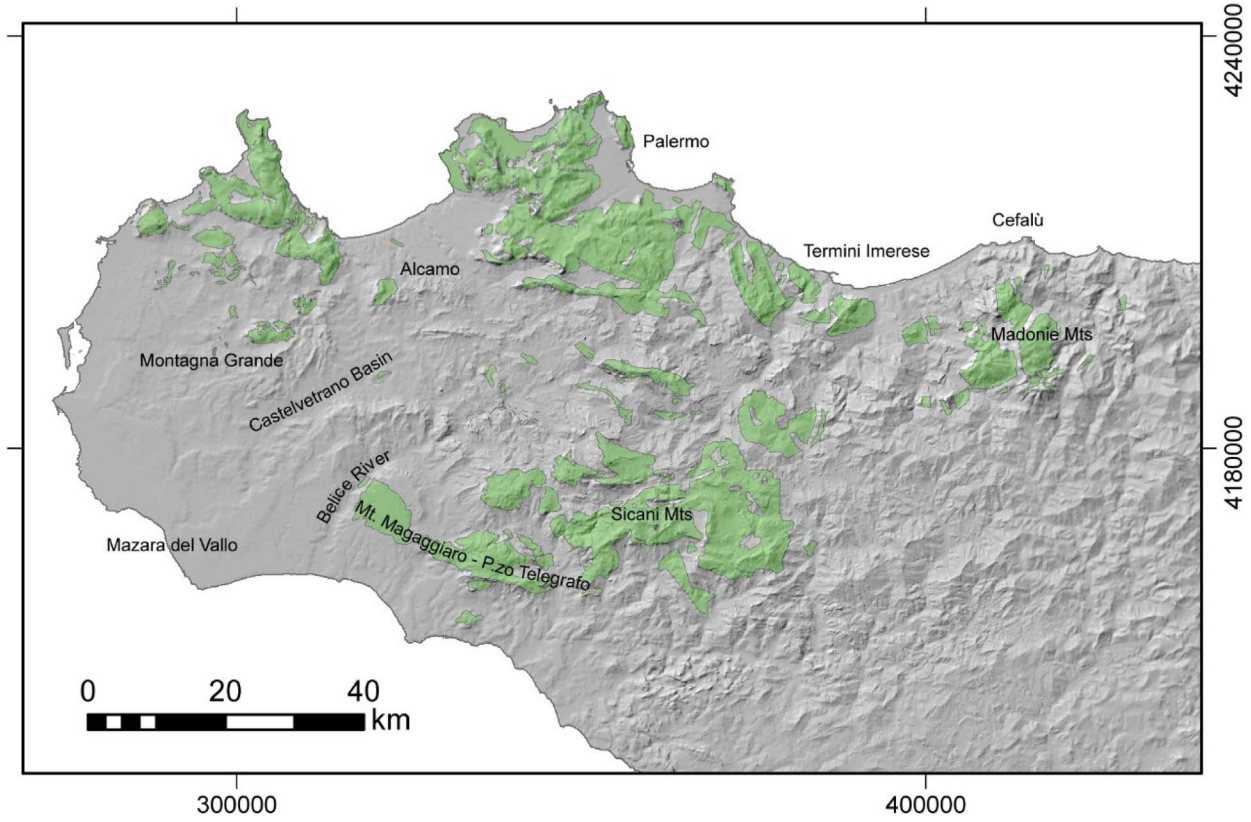

Fig. 12. Areas in which the top of the geothermal reservoir matches the topography.

Ra < 0.05; O'Nions and Oxburgh, 1988).

At Sciacca, the CO_2, the $\delta^{13}C$ signature of CO_2, the high R/Ra ratio and the relatively small, but existing $\delta^{18}O$ shift in thermal springs all suggest the presence of a deep geothermal reservoir. As the volcanic centre that formed the isle of Ferdinandea in the 19th century is only 20 km offshore from Sciacca (Fig. 1), it is reasonable to suppose that the mantle magma that produce ^3He and the geothermal systems that produce hydrothermal CO_2 is located offshore. If this is the case, it is likely that the thermal water from the Selinuntine spring comes from a tectonic structure with convective circulation prevalently offshore.

4. 3D reconstruction of structural geometries at depth

The backbone of Western Sicily is mostly composed of a Meso-Cenozoic shelf and deep-water carbonates. These units were found to be tectonically thickened and uplifted in the northern - more deformed - sectors where these units widely crop out, while in the south-western sector they were buried under the *syn*-tectonic clastic deposits filling the Castelvetrano Basin (Fig. 2) (e.g. Catalano et al., 2002). In SW Sicily these units, which host the regional geothermal reservoirs (Fancelli et al., 1991; Montanari et al., 2015), were only encountered in deep wells and imaged by seismic reflection profiles. South of the Belice river, these units crop out again in at the Mt. Magaggiaro-Pizzo Telegrafo ridge (Catalano et al., 2000) (Figs. 2 and 12). To reconstruct the attitude at depth (isobaths) of these units, we integrated all the available geological and geophysical data (Fig. 13), which were mainly produced within the framework of previous oil and gas explorations, such as seismic reflection profiles and deep wells (Catalano et al., 1995; Catalano et al., 1998; Catalano et al., 2002).

Although it did not produce satisfactory results for the oil and gas industry, this hydrocarbon exploration provided a large amount of useful data for geothermal exploration. The seismic reflection data as well as deep wells were unevenly distributed in the area (e.g. Montanari et al., 2015). We used all the data available in the literature and a confidential dataset kindly provided by Eni S.p.A. for the VIGOR project and located in the SW of the study area. The analysis of the data and their modeling also led to interpretative geological cross sections along the seismic profiles, which were subsequently used for a three-dimensional reconstruction of the top of the regional reservoirs (Figs. 2 and 3). In the sectors where direct information was missing, deep geological cross sections were created on the basis of geological maps. The Bouguer gravity data, generally valid for the interpretations of structures at medium depth, enabled to constrain the trend in depth of the top of the carbonate units For this purpose we used the reconstruction of the buried carbonate units based on geophysical modeling of the available Bouguer and free-air gravimetric data (Carrozzo et al., 1986; ISPRA, ENI, OGS, 2009) by Montanari et al., 2015. These geophysical data were used to extrapolate the top of the carbonate surface where direct information (e.g. well data or even high quality seismic profiles were missing (Montanari et al., 2015).

The 3D geological modeling enabled us to recognize a general spatial continuity of the geological units and to define the deep tectonic structural setting of western Sicily (Fig. 14). This area was found to be characterized at depth by several structural highs and lows although a degree of lateral continuity within the Mesozoic carbonates (i.e. the regional reservoirs) was clearly evident. Due to the characteristics of the dataset, fault surfaces were not modeled however in our opinion this did not particularly affect the surface reconstruction at this regional scale.

In the Mazara del Vallo area, a NE-SW trending structural high was clearly evident, interpretable as a thrust anticline. Moving to the SE, this structure was flanked by another parallel structure developed between Campobello di Mazara and the Castelvetrano Basin (for the location of these places see Fig. 2). These two structures were separated by an elongated deep depression. Barreca et al. (2014) recently reported signs of active tectonic activity related to this latter structure.

To the north, these structures appeared to stop against the Lippone structural high, approximately east-west oriented and interpretable as the result, on a small scale, of the juxtaposition of some lateral thrust ramps. The Lippone high was encountered in oil exploration wells and hosts an exploited gas field within the Miocene terrigenous deposits (Pieri, 2001).

Moving to the north, the top of the carbonate units tends to plunge further, reaching a maximum depth (over 4000 m below sea level) and then rising quickly in the Montagna Grande area (Figs. 2 and 15), where these units come to the surface in the hanging wall of a main thrust fault developed on a regional scale (Catalano et al., 2002).

Using the same approach, the top of the crystalline basement was mapped by integrating the available data in the literature. Due to the lack of direct well data, we achieved a first-order approximation of the 3D geometry, mainly based on indirect geophysical data.

The main input data, used as a benchmark for the 3D reconstruction, was the top of the magnetic basement as interpreted from magnetic data by Cassano et al. (1986). The concept of a magnetic basement is related to the high-to-intermediate magnetic susceptibility of crystalline rocks compared to the low susceptibility of sedimentary

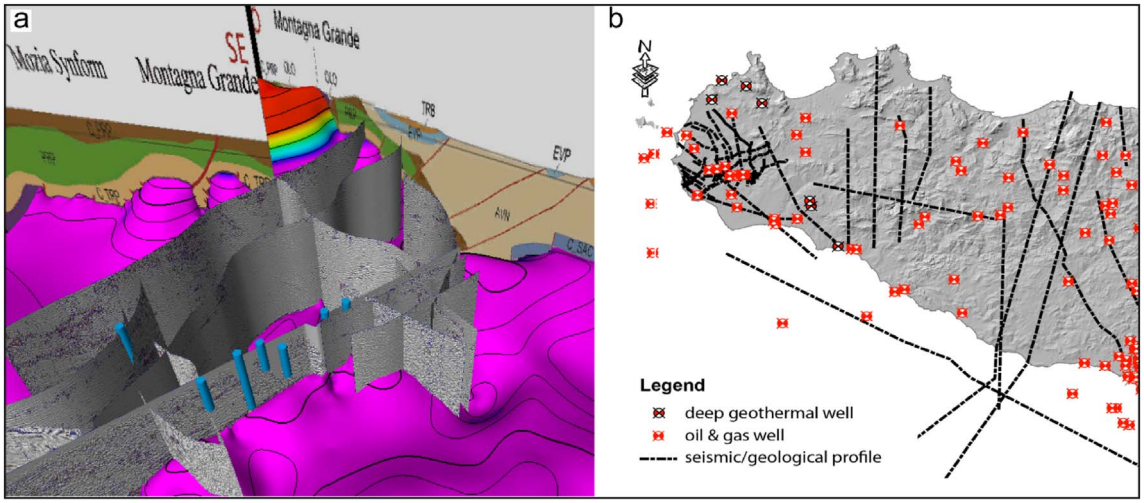

Fig. 13. a) Exemplificative view of the integration between different data (borehole stratigraphy, seismic profiles, and geological cross sections) during the 3D modeling; the mainly purple surface represents the top reservoir surface during a step of the modeling approach. b) Base map showing the location of wells, traces of geological cross sections and seismic profiles used for the reconstruction of the top of the geothermal reservoir surface (modified after Montanari et al., 2015). (For interpretation of the references to color in this figure legend, the reader is referred to the web version of this article.)

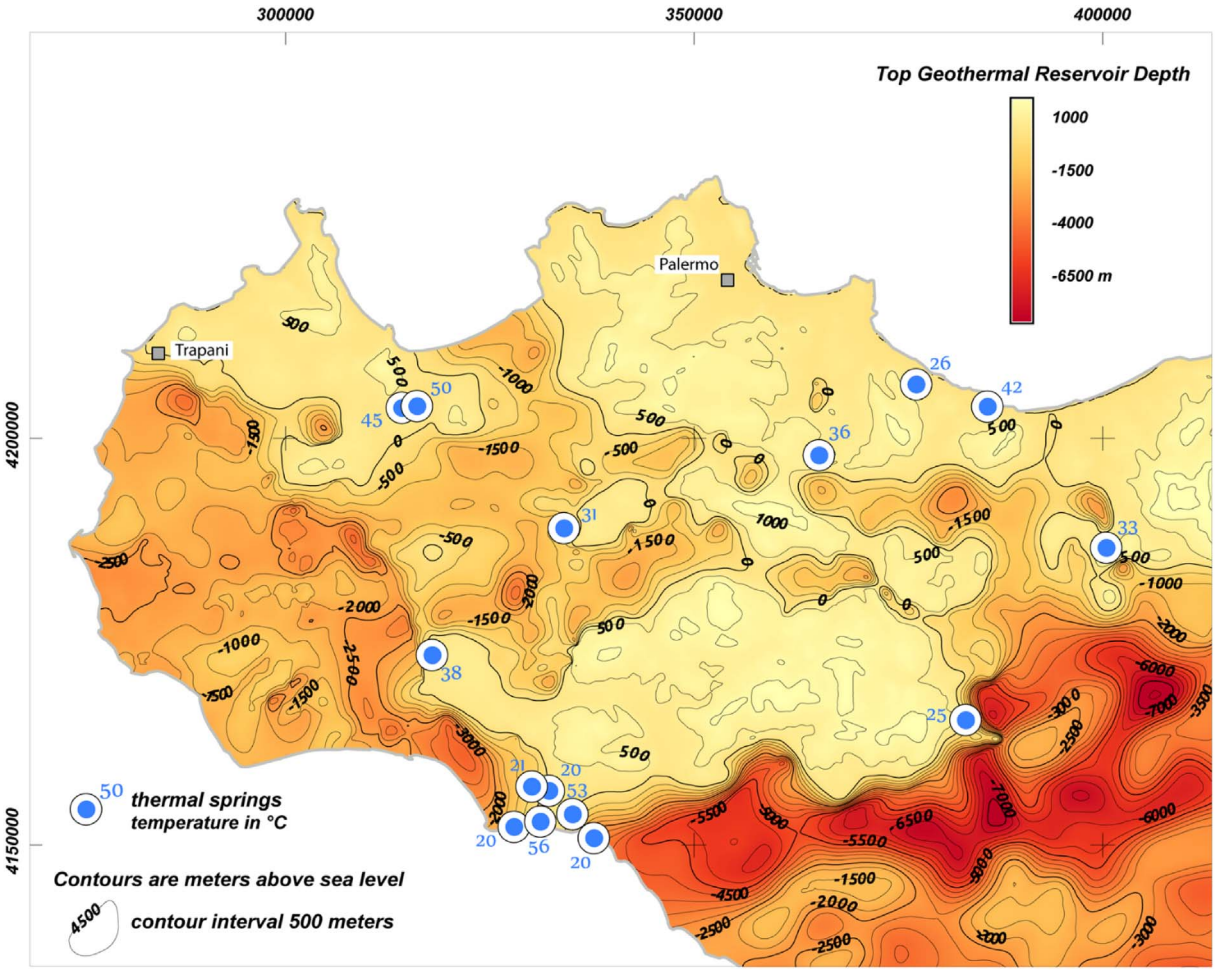

Fig. 14. Contour map of the top of the regional reservoir, the thermal springs are also located with the relative temperature (adapted from Montanari et al., 2015).

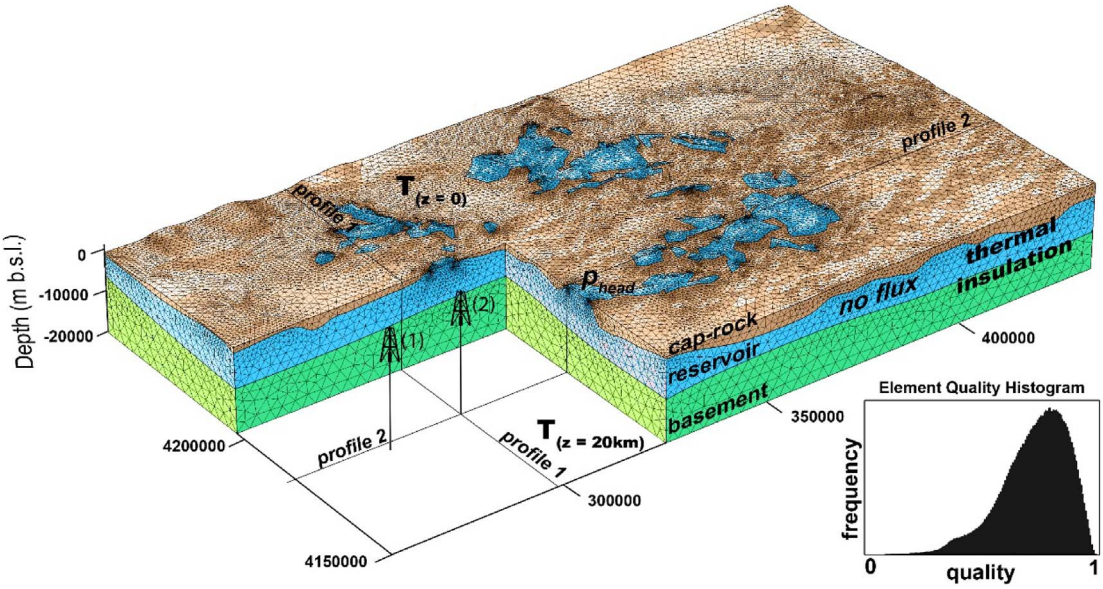

Fig. 15. Geological and physical features used as inputs to solve the numerical model. The three lithothermal units are the impervious sedimentary cover unit (brown), the carbonate reservoir unit (blue) and the magnetic basement unit (green). As thermal boundary conditions, thermal insulation on vertical walls and fixed temperatures at the upper (T_o) and lower ($T_{z=20km}$) surfaces are used. The settings of the fluid dynamic model consist in no-flow boundary conditions applied to the buried reservoir walls and the freshwater head (p_{head}) where the reservoir unit crops out. The subplot in the lower-right corner displays the mesh element quality histogram. The traces of the vertical profiles in Fig. 6 and cross sections in Fig. 16 are reported. (For interpretation of the references to color in this figure legend, the reader is referred to the web version of this article.)

Table 3a
Physical parameters of the lithothermal units.

	Symbol	Cap-rock	Reservoir	Basement	Reference
Physical parameter					
Matrix thermal conductivity	k_{mo} [W/(m K)]	2.0	3.8	3.0	This study
Heat production	A [μW/m^3]	1.5	0.5	3.0	This study
Surface porosity	ϕ_o	0.3	0.1	0.001	This study
Compaction factor	c [1/km]	0.5	0.4	–	This study
Superficial permeability	K_o [m^2]	–	10^{-16}–10^{-13}	–	This study
Skin depth	d [m]	–	1000	–	Ebigbo et al. (2014)
Other constants					
Standard gravity	g [m/s^2]	9.81			
Standard temperature	T_{ref} [°C]	20			
Standard pressure	p_o [Pa]	$\sim 10^5$			
Average soil temperature	T_{av} [°C]	18			Galgaro et al. (2012)
Thermal lapse rate	G_{th} [°C/km]	6.4			
Thermal conductivity correction factors	T_M [°C]	1200			Sekiguchi (1984)
	k_M [W/(m K)]	1.8418			Sekiguchi (1984)

Table 3b
Constitutive laws used to describe the macroscopic behavior of the water-rock system.

Material	Variable	Constitutive law	Reference
Water thermal conductivity	$k_w(T)$	3th order-polynomial function valid in the temperature range 0–280 °C.	Poling et al. (2001)
Water density	$\rho_w(T)$	3th order-polynomial function valid in the temperature range 0–280 °C.	Poling et al. (2001)
Water viscosity	$\eta(T)$	6th and 3th order-polynomial functions valid in the temperature range 0–140 °C and 140–280 °C, respectively.	Poling et al. (2001)
Rock porosity	$\phi(z)$	$\varphi(z) = \varphi_o \exp(-c \cdot z)$	Pasquale et al. (2011)
Matrix thermal conductivity	$k_m(T)$	$k_m(T) = k_M + \left[\frac{T_{ref} T_M}{T_M - T_{ref}} \cdot (k_{mo} - k_M) \cdot \left(\frac{1}{T} - \frac{1}{T_M}\right)\right]$	Sekiguchi (1984)
Effective thermal conductivity	$k_{eff}(T,z)$	$k_{eff}(T,z) = k_m(T)^{(1-\varphi(z))} \cdot k_w(T)^{\varphi(z)}$	Pasquale et al. (2011)
Permeability	$K(z)$	$K(z) = K_o \exp(-z/d)$	Ebigbo et al. (2014)

Table 3c
Equation form of the thermal and fluid flow boundary conditions applied in this study.

Model	Boundary	Boundary condition	Equation	Note
Thermal	Upper surface	Dirichlet	$T_o(z) = T_{av} - G_{th} \times z$	
	Lower surface	Dirichlet	$T_{20km} = 300$–500 °C	
	Vertical walls	Thermal insulation	$-\mathrm{n} \cdot (-k \nabla T) = 0$	**u** is the normal vector
Fluid flow	Reservoir outcrops	Pressure, no viscous stress	$\mathrm{n}^{\mathrm{T}} \cdot [p_o + \eta \cdot (\nabla \mathrm{u} + (\nabla \mathrm{u})^T)] \cdot \mathrm{n} = -f_o$ with **u** the fluid velocity field	f_o is the freshwater head
	Surfaces	No-slip	$\mathbf{u} = 0$	
	Point	Pressure constraint	$p = p(z)$	Hydrostatic profile

rocks. In addition, we also integrated the few interpreted seismic profiles imaging the seismic crystalline basement (e.g. Catalano et al., 1996). The two datasets were comparable and suitable for an integrated analysis.

The three-dimensional geophysical data integration, geological modeling and mapping were carried out using “PETREL” software (Schlumberger).

5. Thermal modeling

In our model, the geothermal system of western Sicily is described by the combination of flow and heat transport equations over a 3D domain of 175 × 100 × 20 km^3. The differential equations are approximated through the finite element method on a tetrahedral mesh grid counting > 10^6 nodes. Given that our goal is to reproduce the actual temperature field of the geothermal reservoir, the time-dependent terms of the balance equations were neglected in order to obtain the steady-state solution. The geological and physical features used as inputs to solve the numerical model are described below and shown in Fig. 15.

The geometrical model considers three main lithothermal units, from the top to the bottom: i) the impervious sedimentary cover unit acting as a cap-rock, ii) the tectonically thickened carbonate units hosting the main regional reservoir, and iii) the basement unit (see Section 4 for details of the reconstruction of the top of these units). Each lithothermal unit is composed of different rocks with similar thermal and hydraulic properties. The rocks were treated as a homogeneous and downward anisotropic porous material. Mixing laws were applied to estimate the effective thermal and hydraulic properties of the rock-water system accounting for the in situ conditions (depth and temperature). The physical parameters and the set of constitutive laws used to characterize the macroscopic behavior of the lithothermal units are summarized in Tables 3a and 3b.

Since the cap-rock and the basement units consist of mainly impermeable rocks, we evaluated the thermal effects of the interplay of the free convection and topographically driven groundwater flow in the permeable reservoir domain. The fluid-velocity and the pore-pressure fields in the impermeable units are fixed to zero and follow a hydrostatic profile, respectively. In those domains, the fluid is stationary and a purely conductive heat transport then takes place. Instead, in the carbonate reservoir, regional hydraulic gradients and hydrothermal convection affect the temperature field by mass and energy transport. A volume force term is added in the momentum equation to include the contribution of gravity and thermal buoyancy.

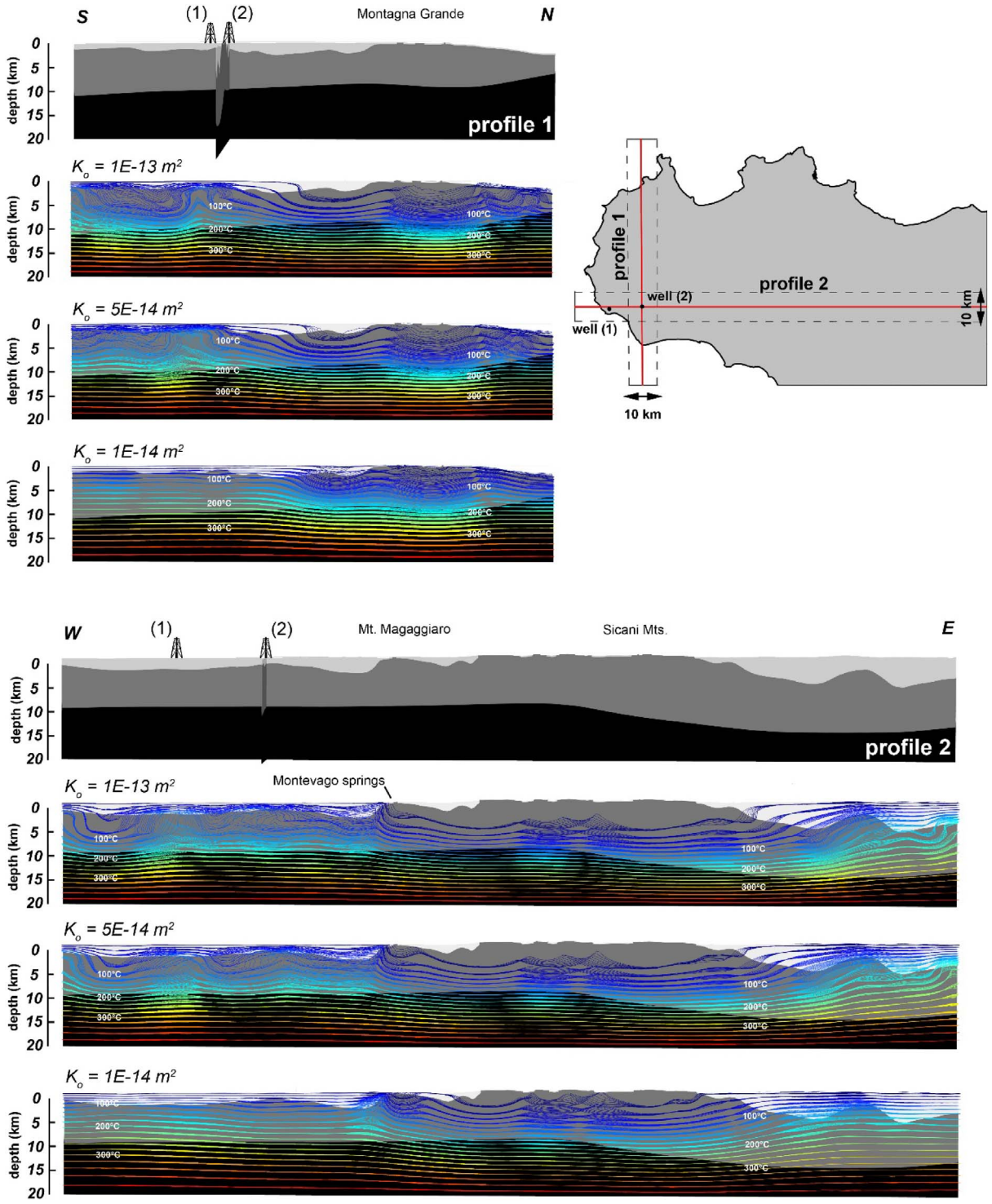

Fig. 16. Geological cross sections and superimposed simulated temperature distributions for a fixed basal temperature of 400 °C and reservoir permeability increasing from $1{\cdot}10^{-14}$ m² to $1{\cdot}10^{-13}$ m². The locations of the two deep boreholes discussed in the text are also reported.

The buried upper and basal boundaries of the reservoir are impermeable to fluid flow, allowing only conductive heat transfer. Accounting for the recharge zones, we applied a stress boundary condition where the reservoir units crop out. As the reservoir is assumed to be fully saturated, the pressure on those boundaries is set as equal to the freshwater head calculated with a reference water density of 1000 kg/m³ and the sea level as datum. Regarding the upper and lower thermal boundaries, we defined the mean annual soil temperature (Table 3a) and a specific isotherm at 20 km depth, respectively. The vertical boundaries surrounding the 3D block multi-layers do not allow a horizontal flow of fluid and heat. The equation form of the thermal and fluid flow boundary conditions used here are summarized in Table 3c.

As physical assumptions regarding rock properties and boundary conditions often suffer from large uncertainties, different scenarios varying the reservoir hydraulic permeability and thermal constraint have been evaluated. The scheme of the parametric study consists in several solutions resulting from all the combinations of the permeability values and basal temperature varying in the range 10^{-16}–10^{-13} m² and 300–500 °C, respectively. Fig. 16 shows the simulated temperature

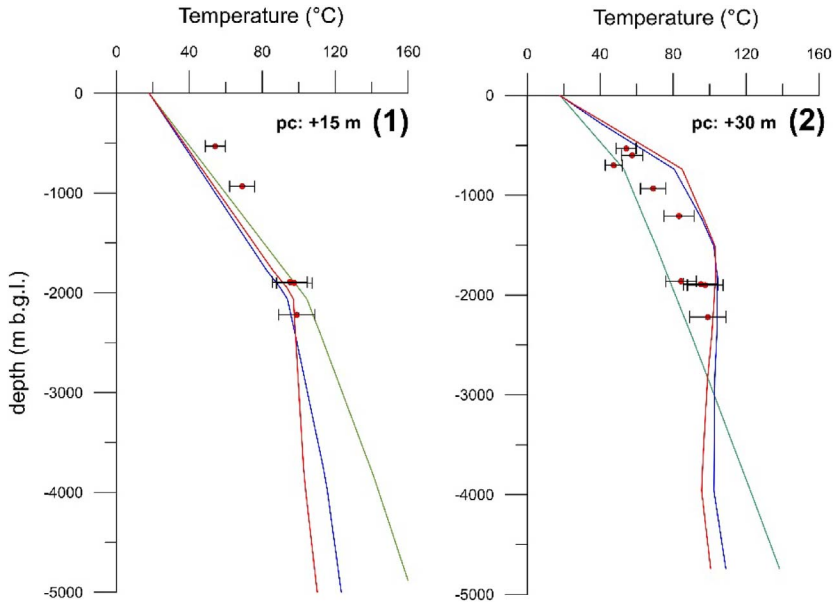

Fig. 17. Simulated temperature profiles together with the corrected BHTs of the two deep boreholes (see Fig. 16 for their location). The curves represent the vertical thermal profiles evaluated with a basal temperature of 400 °C and reservoir permeability equal to $1{\cdot}10^{-14}$ m^2 (green), $5{\cdot}10^{-14}$ m^2 (blue) and $1{\cdot}10^{-13}$ m^2 (red). (For interpretation of the references to color in this figure legend, the reader is referred to the web version of this article.)

distributions for a fixed basal temperature of 400 °C and increasing reservoir permeability along two cross-sections (see also Fig. 12 for their location).

The fluid flow towards the local groundwater base level causes the upwelling of the isotherms locally (Fig. 16). High superficial geothermal gradients characterize these sectors, nevertheless the temperatures do not exceed 40–50 °C because of the shallowness of the processes. With a superficial reservoir permeability lower than or equal to $1 \cdot 10^{-14}$ m^2, the thermal anomalies due to free convection cannot develop, and the deep temperature field is mainly controlled by the conductive heat transfer (Fig. 16). Convection cells develop by increasing the hydraulic permeability.

A minimum misfit between simulated and measured temperatures was found for a reservoir hydraulic permeability of $5 \cdot 10^{-14}$ m^2 and a fixed basal temperature of 400 °C. Thermal data, mainly bottom-hole temperatures (BHT) measured deep hydrocarbon exploratory wells (Fig. 4 and Appendix A), were used as control points on which the overall best fit was assessed.

The thermal effects due to the drilling were evaluated in order to correct the BHTs (Pasquale et al., 2008, Trumpy et al., 2015). Although the quality of the thermal data was also generally low with a mean error of the order of ± 10%, the dataset was adequate to highlight the main regional thermal anomalies. The BHTs measured in the boreholes that had intercepted the deep-seated reservoir highlighted the thermal anomalies, especially in the southwestern area.

The upwelling of hot fluids generates localized thermal anomalies with a characteristic thermal feature: i) a high geothermal gradient in the impermeable cover unit, and ii) a lower gradient in the deep-seated geothermal reservoir. As the vertical thermal conductivity contrast did not justify such a vertical thermal gradient difference in all places, this variation was related to convective processes occurring in the carbonate reservoir (Trumpy et al., 2015). Fig. 17 shows the simulated temperature profiles of Contrada Triglia (number 1), and Gazzera (number 2) wells together with the corrected BHT data. The well locations are reported in Figs. 15 and 17.

6. Discussion

Our review of geological data highlighted that away from their outcrops the carbonate units irregularly deepen towards the south-west up to a depth of about 2000 m.b.s.l. in the Mazara del Vallo area (Figs. 4 and 12), and reaching greater depths in the central part of the study area due to tectonics that heavily affected the area (Fig. 14). From a geometrical point of view, these units exhibit a general lateral continuity at depth along the whole area, suggesting the potential regional extent of the geothermal reservoir.

An analysis of reliable altitude-water isotopes signatures (Fig. 9b), highlights the presence of an effective regional groundwater flow within the carbonate units, which acts as a regional reservoir.

Indeed, groundwater flow paths that extend for 30–40 km are necessary to justify the average recharge elevation in the range of 600–750 m a.s.l. found for some thermal springs (e.g., Segestane and Montevago), given the altitudes of such springs and the morphology of western Sicily. By crossing morphological and geological data, we determined that the recharge of the regional reservoir mainly occurs in the Sicani and Montagna Grande Mts, where carbonate units widely crop out (Fig. 12). Also, the lack of tritium and the high flow rates of such springs are congruent with this groundwater flow system arrangement.

From the regional analysis of the temperature data and spring occurrences, similar features were recognized inside the various portions of the regional carbonate reservoir. Cold temperatures and very low gradients characterized the thermal profiles in the proximal sectors of the geothermal system (Figs. 5, 18 and 19) where carbonate units widely crop out (Fig. 12).

Due to the water rising towards the groundwater base level, both cold and thermal springs occur at the boundary between carbonates and cap-rock units. For example, one of the main hydrothermal manifestations in western Sicily is the Montevago spring (Figs. 2, 14 and Table 2), which is located close to some cold springs at the western border of the Mt Magaggiaro carbonate outcrop, where the total groundwater outflow was estimated to be about 320 L/s by Monteleone and Pipitone (1991).

The physical and chemical features of the Montevago spring, i.e. temperatures in the interval 31–41 °C and electrical conductivity of 1500–2560 S/cm (Alaimo et al., 1978; Alaimo et al., 1990; Catalano et al., 1982; Dall'Aglio and Tedesco, 1968; Fancelli et al., 1991; Favara et al., 2001; Grassa et al., 2006; Santilano et al., 2016), suggest the occurrence of mixing processes between the shallow freshwater and hot deep fluids. The results of the thermal model (Fig. 16) support this

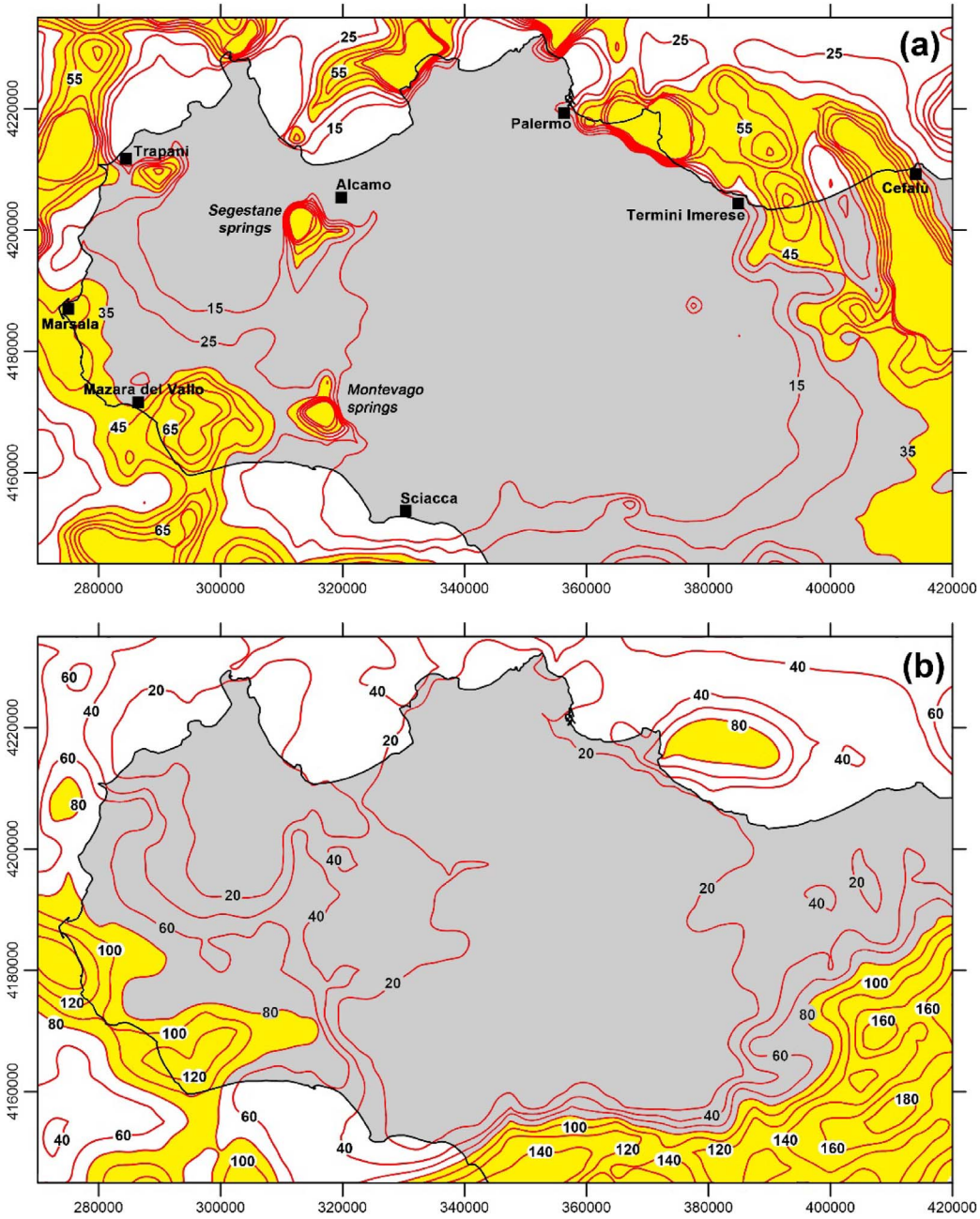

Fig. 18. Maps of the geothermal gradient (a) and the estimated temperature at the top of the carbonate unit (b) with isoline steps of 10 mK/m and 20 °C, respectively.

finding. Indeed, in the base level zone of the carbonate outcrop, the model highlights an isotherms upraising which is linked to the arrival of deep groundwater. At the same time, the shape of the colder isotherms highlights the occurrence of local water infiltration within the carbonate reservoir and its influence on the hot water coming up from the depths.

In addition to the regional groundwater flow provided by the effect of topographic relief, convection takes place in the distal part of the reservoir (i.e. in the south-western sectors, Fig. 19), far from the Mesozoic carbonate outcrops. In these sectors, the numerical model reproduced the thermal anomalies, thus highlighting the role of thermally-driven convection (Figs. 18 and 19). Fig. 18 a and b show the computed shallow geothermal gradients and the estimated temperature at the top of the carbonate unit respectively. At a regional scale, geothermal gradients higher than 35 °C/km (i.e. higher than the mean regional geothermal gradient) characterize many parts of the studied area.

A wide NW-SE trending anomaly is concentrated in the south-western sector with higher values of thermal gradient and temperature at the top of reservoir in the Gazzera-Campobello structural highs (to the SE of Mazara del Vallo). Looking in detail at this thermal anomaly, the apparent NW-SE trend (Fig. 18b) could be related to the coalescence of distinct smaller thermal anomalies, probably associated with the structural highs (see Fig. 1) connecting this portion of Sicily with the Sicily Channel. These thrust-related structural highs also overlap with the areas where signs of magmatic activity were also recorded (such as the ephemeral volcanic island Ferdinandea shown in Fig. 1). Anomalous geothermal gradients also occurred in the well-known Termini-Imerese hydrothermal area located in the north eastern sector. Here, the thermal anomaly affects the off-shore region and extends on-land towards the Cefalù-Madonie Mts zone (Fig. 18a).

Regarding the Sciacca hydrothermal system, the regional model did not reproduce the observed anomaly, merely reproducing the influx of cold water from north-eastern sectors (Fig. 18), and probably mixing

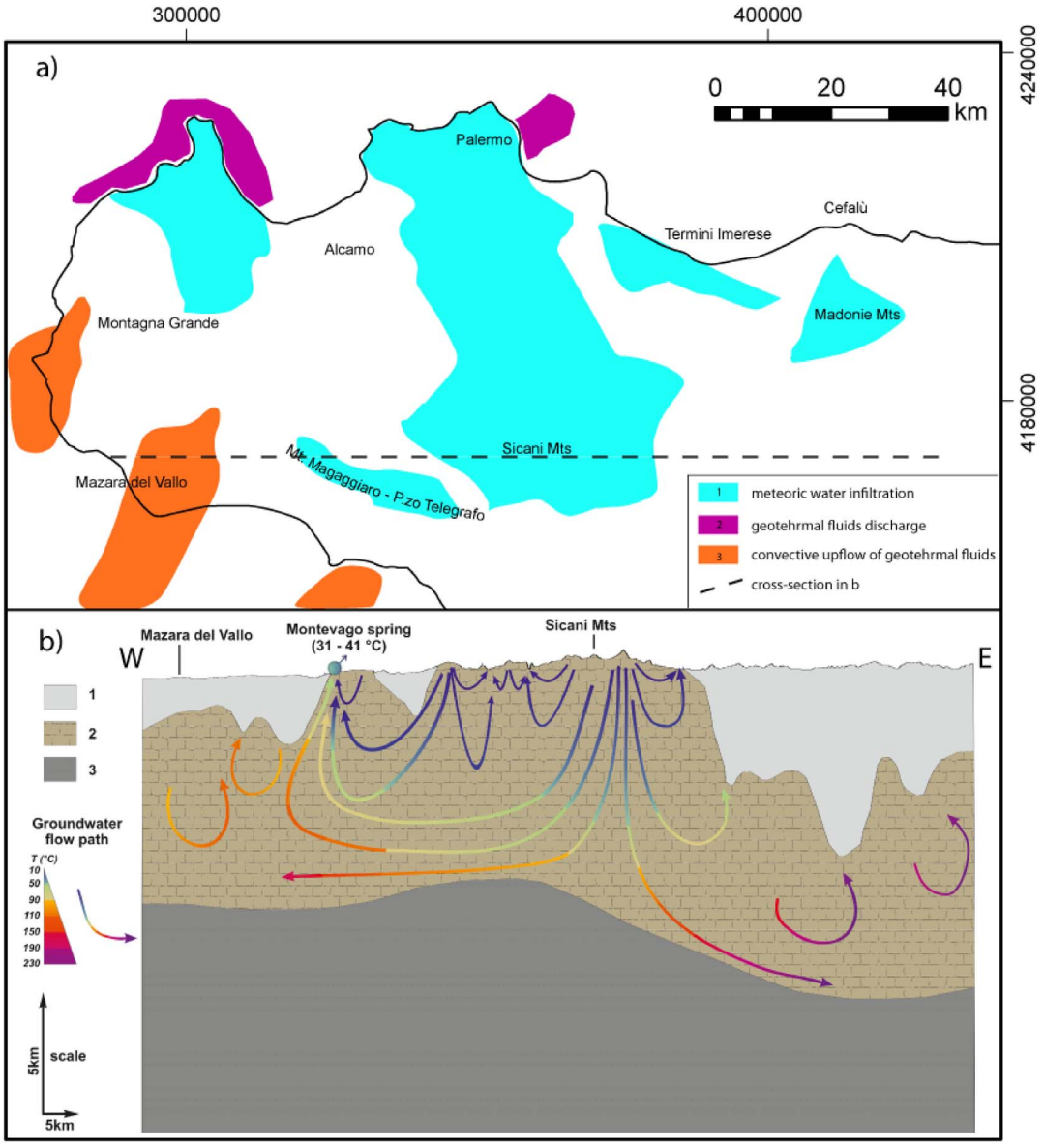

Fig. 19. Conceptual model of groundwater flow within the carbonate reservoir in western Sicily. a) Sketch map: 1) main recharge areas of the carbonate reservoir; 2) offshore zones of geothermal fluids discharge (after Catalano et al., 1988); 3) convective geothermal flow zones; b) cross section: 1) cover; 2) carbonate reservoir; 3) basement.

with the thermal fluids rising up from deeper levels. One possible reason is that the Sciacca hydrothermal system could be related to a sub-vertical tectonic structure which may play an important role in the fluid path, which was not reproduced in the simplified numerical model. However, in the south eastern adjacent sector, as the reservoir abruptly goes down to over a 4 km depth, temperatures as high as 120–140 °C are predicted (Fig. 18). Geochemical evidence, in particular the high $^{3}He/^{4}He$ ratio of discharging fluids reveals the deep origin of the Sciacca hydrothermal system. Likely, the hot fluids circulate at depths of several kilometers and move to the surface along the structure affecting the carbonate units (Fig. 18 and Table 2). In a similar fashion as assumed for the Mazara del Vallo area, also possibly in this case, the N-S oriented structural highs depicted in Fig. 1 could play an active role, channeling the rising up of these thermal fluids.

7. Conclusions

Deciphering the dimension and behavior of a regional-scale geothermal system is generally not easy, because of the lack of evenly distributed data, and because it is easier to study the individual or few fluid occurrences (springs or alimentation areas) as distinct and isolated systems. This is especially true when working in extended areas and structurally complex contexts as in western Sicily. Dealing with carbonate-hosted geothermal systems further complicates the matter due to the complexity of the fracture dominated secondary permeability patterns. In order to unravel such a complex geothermal system, we have demonstrated the advantages of an integrated approach combining geological, geophysical and hydro-geochemical data.

The main conclusions can be summarized as follows:

- Data collected in western-Sicily enabled us to reconstruct the distribution and to verify the lateral continuity at depth of Mesozoic carbonates;
- The water isotopes of cold and thermal springs enabled us to confidently evaluate the average altitudes of recharge for the groundwater hosted within the geothermal reservoir. It was also possible to gain an insight into the water residence times. Both these results, in agreement with water and gas chemistry, suggested the presence of wide groundwater flow systems in the reservoir and a continuity of the latter beneath the impervious caprocks;

- We identified the main recharge areas of the geothermal system on the higher reliefs in the carbonate outcrops;
- Within the carbonate rocks, we reconstructed a homogeneous gradient of temperature (about 10 °C/km) and a temperature increase moving away from the carbonate outcrops (30–40 °C) towards distal and confined parts (up to 140 °C) of these hydro-geological complexes;
- In addition to the regional groundwater flow provided by the effect of topographic relief, thermally-driven convection take place in the distal part of the reservoir;
- Based on all this information, in W-Sicily an extensive regional scale reservoir made up of carbonate complexes and hosting a middle enthalpy geothermal resource can be reconstructed;
- The active fault zone that facilitates a significant geothermal fluid ascent from depth, as well as the presence of a magma chamber which may be present at some depth in the area (Caracausi et al., 2005; Di Stefano et al., 2015), although they cannot be completely ruled out, do not appear to be required to sustain the regional fluid circulation model we depicted (with the exception of the Sciacca area as discussed).

In our opinion the approach used to reconstruct geothermal fluid circulation on a regional scale and the reconstructed circulation modalities, could be taken as illustrative of the general behavior of low-to-medium enthalpy geothermal systems hosted in carbonate units, which can attain huge lateral and vertical dimensions.

Supplementary data to this article can be found online at http://dx.doi.org/10.1016/j.earscirev.2017.04.016.

Acknowledgements

We wish to acknowledge to two anonymous reviewers for their helpful suggestion, which helped improving the manuscript. This research was performed within the framework of the VIGOR Project, aimed at assessing the geothermal potential and exploring the geothermal resources of four regions in southern Italy. VIGOR is part of the activities of the Interregional Programme “Renewable Energies and Energy Savings FESR 2007-2013 – Axes I Activity line 1.4 “Experimental Actions in Geothermal Energy”. The authors acknowledge the management of the VIGOR Project, and in particular Dr. Piezzo of MiSE-DGENRE (Directorate General for Nuclear Energy, Renewable Energy and Energy Efficiency of the Ministry for Economic Development) and Dr. Brugnoli, Director of CNR-DTA (National Research Council of Italy, Department of Sciences of the Earth System and Environmental Technologies). The authors are also grateful to Raimondo Catalano, Salvatore Monteleone and Antonio Contino (Palermo University) for their assistance in addressing the regional geology in western Sicily, also providing data and interpretations.

References

Abate, S., Albanese, C., Angelino, A., Balasco, M., Bambina, B., Bellani, S., Bertini, G., Botteghi, S., Bruno, P.P., Caielli, G., Caiozzi, F., Calvanese, L., Calvi, E., Caputi, A., Cardellicchio, N., Catalano, R., Catania, M., Contino, A., De Franco, R., De Rosa, D., Desiderio, G., Destro, E., Di Fiore, V., Di Sipio, E., Donato, A., Doveri, M., Fedi, M., Ferrari, E., di Gregorio, G., di Leo, M., Galgaro, A., Gennaro, C., Gianelli, G., Gibilaro, C., Giocoli, A., Giorgi, C., Gola, G., Gueguen, E., Iorio, M., La Manna, M., Lavarone, M., Lombardo, G., Maggi, S., Manzella, A., Maraio, S., Menghini, A., Minissale, A., Montanari, D., Montegrossi, G., Monteleone, S., Mussi, M., Norini, G., Pelosi, N., Perrone, A., Piemonte, C., Pierini, S., Piscitelli, S., Punzo, M., Rizzo, E., Romano, G., Sabatino, M., Santilano, A., Scotto di Vettimo, P., Tamburrino, S., Tarallo, D., Teza, G., Tranchida, G., Trifirò, S., Trumpy, E., Varriale, F., Viezzoli, A., e Votta, M., 2015. VIGOR: Sviluppo geotermico nella regione Sicilia – Studi di fattibilità a Mazara del Vallo e Termini Imerese, Valutazione geotermica con geofisica elitrasportata. Progetto VIGOR – Valutazione del Potenziale Geotermico delle Regioni della Convergenza, POI Energie Rinnovabili e Risparmio Energetico 2007–2013. (CNR-IGG, ISBN: 9788879580175).

Accaino, F., Catalano, R., Di Marzo, L., Giustiniani, M., Tinivella, U., Nicolich, R., Sulli, A., Valenti, V., Manetti, P., 2011. A crustal seismic profile across Sicily. Tectonophysics 508, 52–61.

Alaimo, R., 1984a. Il bacino idrotermale di Sciacca. Nota I: Inquadramento idrogeologico e caratteristiche chimiche delle acque. Risorse Termali della Sicilia, Univ. di Palermo. pp. 141–151.

Alaimo, R., 1984b. Il bacino idrotermale di Sciacca. Nota II: Origine dell'acqua termale. Risorse Termali della Sicilia, Univ. di Palermo. pp. 193–209.

Alaimo, R., Tonani, F., 1984. Il bacino termale di Sciacca. Nota III: Geotermometria delle acque termali e modello di miscuglio per le acque emergenti. Risorse Termali della Sicilia, Univ. di Palermo. pp. 211–225.

Alaimo, R., Carapezza, M., Dongarrà, G., Hauser, S., 1978. Geochimica delle sorgenti termali siciliane. Rend. Soc. Ital. Mineral. Petrol. 34, 577–590.

Alaimo, R., Calderone, S., Inguaggiato, S., Sortino, F., 1990. Indagine geochimica sull'acquifero termale della Sicilia occidentale. Geologia ed idrogeologia, Bari. 25. pp. 101–121.

Angelica, C., Bonforte, A., Distefano, G., Serpoelloni, E., Gresta, S., 2013. Seismic potential in Italy from integration and comparison of seismic and geodetic strain rates. Tectonophysics 608, 996–1006. (07/2013). http://dx.doi.org/10.1016/j.tecto.2013.07.014.

Antolini, P., Sommaruga, C., 1953. Considerazioni geologiche sul permesso di ricerca forze endogene “Termini Imerese”, Agip Mineraria, Int. Rep. N. 882 (34pp).

Aureli, A., 1996. Bacino termale di Sciacca (Sicilia S.O.): caratteristiche idrogeologiche e vulnerabilità. CNR, Quaderni di tecniche di Protezione Ambientale. 59 (168pp).

Avanzinelli, et al., 2013. Mantle melting in within-plate continental settings: Sr–Nd–Pb and U-series isotope constraints in alkali basalts from the Sicily Channel (Pantelleria and Linosa Islands, Southern Italy). Lithos 188, 113–129.

Barreca, G., Maesano, F.E., 2012. Restraining stepover deformation superimposed on a previous fold-and-thrust-belt: a case study from the Mt. Kumeta–Rocca Busambra ridges (western Sicily, Italy). J. Geod. 55, 1–17.

Barreca, G., Bruno, V., Cocorullo, C., Cultrera, F., Ferranti, L., Guglielmino, F., Guzzetta, L., Mattia, M., Monaco, C., Pepe, F., 2014. Geodetic and geological evidence of active tectonics in south-western Sicily (Italy). J. Geodyn. 82, 138–149. http://dx.doi.org/10.1016/j.jog.2014.03.004.

Belguith, Y., Geoffroy, L., Mourgues, R., Rigane, A., 2013. Analogue modelling of Late Miocene–Early Quaternary continental crustal extension in the Tunisia–Sicily Channel area. Tectonophysics 608 (576–585) (2006).

Bello, M., Franchino, A., Merlini, S., 2000. Structural model of Eastern Sicily. Mem. Soc. Geol. Ital. 55, 61–70.

Bernoulli, D., 2001. Mesozoic-Tertiary carbonate platforms, slopes and basins of the external Apennines and Sicily. In: VAI, G.B., MARTINI, P. (Eds.), Anatomy of a Orogen: The Apennines and Adjacent Mediterranean Basins. Kluwer Academic Publishers, Dordrecht, pp. 307–325.

Bertini, G., Casini, M., Gianelli, G., Pandeli, E., 2006. Geological structure of along-living geothermal system, Larderello, Italy. Terra Nova 18, 163–169.

Bjornsson, G., Flovenz, O.G., Saemundsson, K., Einarsson, E.M., 2001. Pressure Changes in Icelandic Geothermal Reservoirs Associated With Two Large Earthquakes in June 2000, in Proceedings, 26th Workshop on Geothermal Reservoir Engineering, SGP-TR-168: Stanford, Stanford University, January 29–31. pp. 2001 (122 p).

Bottari, C., Siros, S.C., Teramo, A., 2009. Archeological evidence for destructive earthquakes in Sicily between 400 B.C. and A.D. 600. Geoarcheology 24, 147–175.

Capaccioni, B., Vaselli, O., Tassi, F., Santo, A., Delgado-Huertas, A., 2011. Hydrogeochemistry of the thermal waters from Sciacca geothermal field (Sicily, southern Italy). J. Hydrol. 396, 292–311.

Caracausi, A., Favara, R., Italiano, F., Nuccio, P.M., Paonita, A., Rizzo, A., 2005. Active geodynamics of the central Mediterranean sea: heat and helium evidences for a trans-tensional zone connecting the Sicily Channel to the southern Tyrrhenian Sea. Geophys. Res. Lett. 32, L04312. http://dx.doi.org/10.1029/2004GL021608.

Carapezza, M., Cusimano, G., Liguori, V., Alaimo, R., Dongarrà, G., Hauser, S., 1977. Nota introduttiva allo studio delle sorgenti termali dell'isola di Sicilia. Boll. Soc. Geol. Ital. 96, 813–836.

Carrozzo, M.T., Luzio, D., Margiotta C. & Quarta T., 1986. Gravity Anomaly Map of Italy. CNR: “Progetto Finalizzato Geodinamica” – Sottoprogetto: “Modello Strutturale Tridimensionale”.

Cassano, E., Fichera, R., Arisi, Rota F., 1986. Rilievo aeromagnetico d'Italia: alcuni risultati interpretativi. Atti del 5° convegno annuale del Gruppo Nazionale di Geofisica della Terra Solida. pp. 939–962.

Catalano, R., Macaluso, T., Monteleone, S., Calandra, D., 1982. Lineamenti geostrutturali, idrogeologici e geotermici della Sicilia occidentale. Contributo alla conoscenza delle risorse geotermiche del territorio italiano-Progetto finalizzato energetica. 1982. pp. 110–120.

Catalano, R., Cusimano, G., Grasso, M., Lentini, F., Macaluso, T., Monaco, P., Monteleone, S., Pipitone, G., 1988. Inventario delle risorse geotermiche nazionali. Regione Sicilia. Principali strutture idrogeologiche della Sicilia. C. N. R., Istituto internazionale per le ricerche geotermiche. (17 pp., tavv., Pisa).

Catalano, R., Di Stefano, P., Vitale, F.P., 1995. Structural trends and palaeogeography of the central and western Sicily belt: new insights. Terra Nova 7, 189–199.

Catalano, R., Di Stefano, P., Sulli, A., Vitale, F.P., 1996. Paleogeography and structure of the Central Mediterranean: Sicily and its offshore area. Tectonophysics 260, 291–323.

Catalano, R., Franchino, A., Merlini, S., Sulli, A., 1998. Assetto Strutturale Profondo della Sicilia Occidentale. Atti del 79° Congresso Nazionale – Società Geologica Italiana 1998. vol. A. pp. 257–260.

Catalano, R., Franchino, A., Merlini, S., Sulli, 2000. Central western Sicily structural setting interpreted from seismic reflection profiles. Mem. Soc. Geol. Ital. 55, 5–16.

Catalano, R., Merlini, S., Sulli, A., 2002. The structure of western Sicily, central Mediterranean. Pet. Geosci. 8, 7–18.

Catalano, R., Valenti, V., Albanese, C., Accaino, F., Sulli, A., Tinivella, U., Gasparo

Morticelli, M., Zanolla, C., Giustiniani, M., 2013. Sicily's fold–thrust belt and slab roll-back: the SI.RI.PRO. Seismic crustal transect. J. Geol. Soc. 170, 451–464. http://dx.doi.org/10.1144/jgs2012-099.
Cataldi, R., Mongelli, F., Squarci, P., Taffi, L., Zito, G., Calore, C., 1995. Geothermal ranking of the Italian territory. Geothermics, vol. 24 (1), 115–129.
Chiodini, G., Allard, P., Caliro, S., Parello, F., 2000. 18-O exchange between steam and CO_2 in volcanic and hydrothermal gases: implications for the source of water. Geochim. Cosmochim. Acta 64, 2478–2488.
Civetta, L., D'Antonio, M., Orsi, G., Tilton, G.R., 1998. The geochemistry of volcanic rocks from Pantelleria Island, Sicily Channel: petrogenesis and characteristics of the mantle source region. J. Petrol. 39, 1453–1491.
Civile, D., Lodolo, E., Caffau, M., Baradello, L., Ben-Avraham, Z., 2016. Anatomy of a submerged archipelago in the Sicilian Channel (central Mediterranean Sea). Geol. Mag. 153 (1), 160–178. (2016). http://dx.doi.org/10.1017/S0016756815000485.
Corti, G., Cuffaro, M., Doglioni, C., Innocenti, F., Manetti, P., 2006. Coexisting geodynamic processes in the Sicily Channel. Geol. Soc. Am. 409, 83–96. (Special paper). http://dx.doi.org/10.1130/2006.2409(05).
Craig, H., 1961. Isotopic variations in meteoric waters. Science 133, 1702–1703.
Curewitz, D., Karson, J.A., 1997. Structural settings of hydrothermal outflow: fracture permeability maintained by fault propagation and interaction. J. Volcanol. Geotherm. Res. 79, 149–168.
Dall'Aglio, M., 1966. Rilievo geochimico della Sicilia occidentale. Riv. Min. Sic. 175–191 (Anno 17, n.100/102).
Dall'Aglio, M., Tedesco, C., 1968. Studio geochimico ed idrogeologico di sorgenti della Sicilia. Riv. Min. Sic. 171–210 (Anno 19, N.112/114).
Bolognesi, D'Amore, F., 1993. Isotopic variation of the hydrothermal system on Vulcano Isl., Italy. Geochim. Cosmochim. Acta 57, 2069–2082.
Della Vedova, B., Bellani, S., Pellis, G., Squarci, P., 2001. Deep temperatures and surface heat flow distribution. In: Vai, G.B., Martini, I.P. (Eds.), Anatomy of an Orogen. The Apennines and Adjacent Mediterranean Basins. Kluwer Acad, Dordrecht, Netherlands, pp. 65–76.
Di Stefano, P., Favara, R., Luzio, D., Renda, P., Cacciatore, M.S., Calò, M., Napoli, G., Parisi, L., Todaro, S., Zarcone, G., 2015. A regional-scale discontinuity in western Sicily revealed by a multidisciplinary approach: a new piece for understanding the geodynamic puzzle of the southern Mediterranean. Tectonics 34, 2067–2085. http://dx.doi.org/10.1002/2014TC003759.
Doveri, M., Grassi, S., 2010. Convective Water Circulation in a Geothermal Island: Pantelleria (Sicily Channel). Short Paper/Poster – SWIM 21 (Salt Water Intrusion Meeting), Azores 2010, June 21–25, 2010. (Short paper (reviewed) in: Proceedings SWIM21) pp. 154–157.
Doveri, M., Mussi, M., 2014. Water isotopes as environmental tracers for conceptual understanding of groundwater flow: an application for fractured aquifer systems in the "Scansano-Magliano in Toscana" area (Southern Tuscany, Italy). Water 6, 2255–2277.
Duan, Z., Pang, Z., Wang, X., 2011. Sustainability of limestone geothermal reservoirs with extended production histories in Beijing and Tianjin, China. Geothermics 40, 125–135.
Duchi, V., Minissale, A., Thompson, M., Campana, M.E., 1994. Geochemistry of thermal fluids on the volcanic isle of Pantelleria, southern Italy. Appl. Geochem. 9, 147–160.
Ebigbo, A., Niederau, J., Marquart, G., Inversi, B., Scrocca, D., Gola, G., Arnold, J., Montegrossi, G., Vogt, C., Pechnig, R., 2014. Evaluation of the Geothermal Energy Potential in the Medium-Enthalpy Reservoir Guardia dei Lombardi, Italy. PROCEEDINGS, Thirty-Ninth Workshop on Geothermal Reservoir Engineering Stanford University, Stanford, California, February 24–26, 2014, SGP-TR-202.
Fancelli, R., Monteleone, S., Nuti, S., Pipitone, G., Rini, S., Taffi, L., 1991. Nuove conoscenze idrogeologiche e geotermiche nella Sicilia occidentale. Geol. Appl. Idrogeol. 24.
Fancelli, R., Nuti, S., Taffi, L., Monteleone, S., Pipitone, G., 1994. Studio idrogeochimico e termico per la valutazione della Sicilia occidentale. Inventraio delle Risorse Geotermiche Nazionali. Ministero dell'industria, del commercio e dell'Artigianato. CNR-Istituto Internazionale per le Ricerche Geotermiche, Pisa.
Farolfi, G., Del Ventisette, C., 2015. Contemporary crustal velocity field in Alpine Mediterranean area of Italy from new geodetic data. GPS Solutions. http://dx.doi.org/10.1007/s10291-015-0481-1.
Favara, R., Grassa, F., Inguaggiato, S., D'Amore, F., 1998. Geochemical and hydrogeological characterization of thermal springs in western Sicily. J. Volcanol. Geotherm. Res. 84, 125–141.
Favara, R., Grassa, F., Inguaggiato, S., Valenza, M., 2001. Hydrogeochemistry and stable isotopes of thermal springs: earthquake-related chemical changes along Belice Fault (western Sicily). Appl. Geochem. 16, 1–17.
Finetti, I.R., Lentini, F., Carbone, S., Del Ben, A., Di Stefano, A., Forlin, E., Guarnieri, P., Pipan, M., Prizzon, A., 2005. Geological outline of Sicily and lithospheric tectono-dynamics of its Tyrrhenian margin from New CROP Seismic Data. In: Finetti, I.R. (Ed.), CROP Project, Deep Seismic Exploration of the Central Mediterranean and Italy. Elsevier, Amsterdam.
Fisher, A., Abrams, L., Busch, W., 1992. Comparison of laboratory and logging data from Leg 129 and the inversion of logs to determine lithology. Proc. Ocean Drill. Program Sci. Results 129, 507–527.
Galgaro, A., Di Sipio, E., Destro, E., Chiesa, S., Uricchio, V.F., Bruno, D., Masciale, R., Lopez, N., Iaquinta, P., Teza, G., Iovine, G., Montanari, D., Manzella, D.A., Soleri, S., Greco, R., Di Bella, G., Monteleone, S., Sabatino, M., Iorio, M., Petruccione, E., Giaretta, A., Tranchida, G., Trumpy, E., Gola, G., D'arpa, S., 2012. Methodological approach for evaluating the geo-exchange potential: VIGOR Project. Acque Sotterranee – Ital. J. Groundw. 2012, 43–53. http://dx.doi.org/10.7343/AS-014-12-0029.
Gat, J.R., Carmi, I., 1970. Evolution of the isotopic composition of atmospheric waters in the Mediterranean Sea area. J. Geophys. Res. 75, 3032–3048.
Geothopica web site, 2012. Italian National Geothermal Database. (online, available from: http://geothopica.igg.cnr.it/, last accessed: 01/14/2014).
Gianbastiani, B.M.S., Tinti, F., Mendrinos, D., Mastrocicco, M., 2014. Energy performance strategies for the large scale introduction of geothermal energy in residential and industrial buildings: the GEO.POWER project. Energy Policy 65, 315–322.
Gino, G.F., Sommaruga, C., 1953. Le manifestazioni idrotermali della Sicilia. Riv. Min. Sic. 22/23, 172–183.
Gola, G., Manzella, A., Trumpy, E., Montanari, D., van Wees, J.D., 2013. Deep-Seated Geothermal Resource Assessment of the VIGOR Project Regions, Italy. European Geothermal Congress 2013, Pisa, Italy, 3–7 June 2013.
Goldscheider, N., Szonyi, J.M., Eross, A., Schill, E., 2010. Review: thermal water resources in carbonate rock aquifers. Hydrogeol. J. 18, 1303–1318.
Gousmania, M., Gasmi, M., Mhamdi, A., Bouri, S., Ben, Dhia H., 2006. Prospection géoélectrique pour l'étude de l'aquifer thermal des calcaires récifaux, Hmeima-Boujabeur (centre ouest de la Tunisie). C.R. Geosciences 338, 1219–1227.
Grassa, F., Capasso, G., Favara, R., Inguaggiato, S., 2006. Chemical and isotopic composition of waters and dissolved gases in some thermal springs of Sicily and adjacent volcanic islands, Italy. Pure Appl. Geophys. 163, 781–807.
Grassi, S., Squarci, P., D'Amore, M., Mussi, M., 1995. Circulation of Thermal Waters on Pantelleria Island (Sicily Channel, Italy). 1995 World Geothermal Congress, Florence (Italy). pp. 703–706.
Henley, R.W., Ellis, A.J., 1983. Geothermal systems ancient and modern: a geochemical overview. Earth-Sci. Rev. 19, 1–50.
Homuth, S., Götz, A.E., Sass, I., 2015. Reservoir characterization of the Upper Jurassic geothermal target formations (Molasse Basin, Germany): role of thermofacies as exploration tool. Geoth. Energ. Sci. 3, 41–49. http://dx.doi.org/10.5194/gtes-3-41-2015.
ISPRA, ENI, OGS, 2009. Cartografia Gravimetrica Digitale d'Italia alla scala 1:250.000.
Lachenbruch, A.H., Brewer, M.C., 1959. Dissipation of the temperature effect of drilling a well in Arctic Alaska. U.S. Geol. Surv. Bull. 1083-C, 73–109.
Lavecchia, G., Frerrarini, F., d Nardis, R., Visini, F., Barbano, M.S., 2007. Active thrusting as a possible seismogenic source in Sicily (Southern Italy): some insights from integrated structural–kinematic and seismological data. Tectonophysics 445, 145–167. http://dx.doi.org/10.1016/j.tecto.2007.07.007.
Lentini, L., Carbone, F., Catalano, S., 1994. Main structural domains of the central Mediterranean region and their Neogene tectonic evolution. Boll. Geofis. Teor. Appl. 36, 141–144.
Liotta, M., Grassa, F., D'Alessandro, W., Favara, R., Gagliano, Candela E., Pisciotta, A., Scaletta, C., 2013. Isotopic composition of precipitation and groundwater in Sicily, Italy. Appl. Geochem. 34, 199–206.
Lotti, B., 1910. Geologia della Toscana. Mem. Descritt. Carta Geol. D'Italia 13, Roma. (484pp).
Minissale, A., 1991. The Larderello geothermal field: a review. Earth Sci. Rev. 31, 133-15.
Minissale, A., 1992. Isotopic composition of natural thermal discharges on Vulcano Isl., Southern Italy. J. Hydrol. 139, 15–25.
Minissale, A., Duchi, V., 1988. Geothermometry on fluids circulating in a carbonate reservoir in north-central Italy. J. Volcanol. Geotherm. Res. 35, 237–252.
Minissale, A., Vaselli, O., 2011. Karst springs as "natural" pluviometers: constraints on the isotopic composition of rainfalls in the Apennines (central Italy). Appl. Geochem. 26, 838–852. http://dx.doi.org/10.1016/j.apgeochem.2011.02.005.
Moeck, I.S., 2014. Catalog of geothermal play types based on geologic controls. Renew. Sust. Energ. Rev. 37, 867–882. http://dx.doi.org/10.1016/j.rser.2014.05.032.
Mohammadi, Z., Bagheri, R., Jahanshahi, R., 2010. Hydrogeochemistry and geothermometry of Changal thermal springs, Zagros region, Iran. Geothermics 39, 242–249.
Monaco, C., Mazzoli, S., Tortorici, L., 1996. Active thrust tectonics in western Sicily (southern Italy): the 1968 Belice earthquake sequence. Terra Nova 8, 372–381.
Montanari, D., Albanese, C., Catalano, R., Contino, A., Fedi, M., Gola, G., Iorio, M., La Manna, M., Monteleone, S., Trumpy, E., Valenti, V., Manzella, A., 2015. Contour map of the top of the regional geothermal reservoir of Sicily (Italy). J. Maps 11, 13–24. http://dx.doi.org/10.1080/17445647.2014.935503.
Monteleone, S., Pipitone, G., 1991. Schema idrogeologico dell'area Monte Magaggiaro e Pizzo Telegrafo (Sicilia Sud-Occidentale). Boll. Soc. Geol. Ital. 110, 155–164.
O'Nions, R.K., Oxburgh, E.R., 1988. Helium volatile fluxes and the development of continental crust. Earth Planet. Sci. Lett. 90, 331–347.
Parello, F., Allard, P., D'Alessandro, W., Federico, C., Jean-Baptoste, P., Catani, O., 2000. Isotope geochemistry of Pantelleria volcanic fluids, Sicily Channel rift: a mantle volatile end member for volcanism in southern Europe. Earth Planet. Sci. Lett. 180, 325–339.
Pasquale, V., Chiozzi, P., Gola, G., Verdoya, M., 2008. Depth-time correction of petroleum bottom-hole temperatures in the Po Plain, Italy. Geophysics 73 (6), 187–196.
Pasquale, V., Gola, G., Chiozzi, P., Verdoya, M., 2011. Thermophysical properties of the Po Basin rocks. Geophys. J. Int. 186, 69–81.
Pasquale, V., Chiozzi, P., Verdoya, M., Gola, G., 2012. Heat flow in the Western Po Basin and the surrounding orogenic belts. Geophys. J. Int. 190, 8–22.
Pasquale, V., Verdoya, M., Chiozzi, P., 2014. Heat flow and geothermal resources in northern Italy. Renew. Sust. Energ. Rev. 36, 277–285. http://dx.doi.org/10.1016/j.rser.2014.04.075.
Pieri, M., 2001. Italian petroleum geology. In: Vai, G.B., Martini, I.P. (Eds.), Anatomy of an Orogen: The Apennines and Adjacent Mediterranean Basins. Kluwer Academic Publishers, Norwell, Massachusetts, pp. 375–400.
Poling, B.E., Prausnitz, J.M., O'Connell, J.P., 2001. The Properties of Gases and Liquids, fifth ed. McGraw-Hill.
Romagnoli, P., Arias, A., Barelli, A., Cei, M., Casini, M., 2010. An updated numerical model of the Larderello–Travale geothermal system, Italy. Geothermics 39 (2010),

292–313. http://dx.doi.org/10.1016/j.geothermics.2010.09.010.
Sani, F., Bonini, M., Montanari, D., Moratti, G., Corti, G., Del Ventisette, C., 2016. The structural evolution of the Radicondoli–Volterra Basin (southern Tuscany, Italy): relationships with magmatism and geothermal implications. Geothermics 59, 38–55. http://dx.doi.org/10.1016/j.geothermics.2015.10.008.
Santilano, A., Donato, A., Galgaro, A., Montanari, A., Menghini, A., Viezzoli, A., Di Sipio, E., Destro, E., Manzella, A., 2016. An integrated 3D approach to assess the geothermal heat-exchange potential: the case study of western Sicily (southern Italy). Renew. Energy 97, 611–624. http://dx.doi.org/10.1016/j.renene.2016.05.072.
Sekiguchi, K., 1984. A method for determining terrestrial heat flow in oil basinal areas. Tectonophysics 103, 67–79.
Sibson, R.H., 1996. Structural permeability of fluid-driven fault-fracture meshes. J. Struct. Geol. 18 (8), 1031–1042.
Simsek, S., 2003. Hydrogeological and isotopic survey of geothermal fields in the Buyuk Menderes graben, Turkey. Geothermics 32, 669–678.
Trumpy, E., Manzella, A., 2017. Geothopica and the interactive analysis and visualization of the updated Italian National Geothermal Database. Int. J. Appl. Earth Obs. Geoinf. 54, 28–37. http://dx.doi.org/10.1016/j.jag.2016.09.004.
Trumpy, E., Donato, A., Gianelli, G., Gola, G., Minissale, A., Montanari, D., Santilano, A., Manzella, A., 2015. Data integration and favourability maps for exploring geothermal systems in Sicily, southern Italy. Geothermics 56 (2015), 1–16. http://dx.doi.org/10.1016/j.geothermics.2015.03.004.
Trumpy, E., Botteghi, S., Caiozzi, F., Donato, A., Gola, G., Montanari, D., Pluymakers, M., Santilano, A., Van Wees, J.D., Manzella, A., 2016. Geothermal potential assessment for a low carbon strategy: a new systematic approach applied in southern Italy. Energy. http://dx.doi.org/10.1016/j.energy.2016.02.144. (2016).
Vai, G.B., 2001. Basement and Early (Pre-Alpine) history. In: Vai, G.B., Martini, P. (Eds.), Anatomy of an Orogen. The Apennines and Adjacent Mediterranean Basins. Kluwer Academic Publish.